博士学位論文

Angular Correlations of the Inflationary Stochastic Gravitational Wave Background

（インフレーションによる確率的な背景重力波の角度相関）

令和５年３月

WU ZHENYUAN

山口大学大学院創成科学研究科

Angular Correlations of the Inflationary Stochastic Gravitational Wave Background

By

Zhen-Yuan Wu

A Thesis
Submitted to Yamaguchi University
in Conformity with the Requirements for
the Degree of Philosophy

Yamaguchi, Japan

2023

TABLE OF CONTENTS

LIST OF FIGURES

LIST OF ABBREVIATIONS

AAC	Antipodal Angular Correlations
BBH	Binary Black Holes
BNS	Binary Neutron Stars
CMB	Cosmic Microwave Background
FLRW	Friedmann-Lemaître-Robertson-Walker
DOF	Degrees of Freedom
GWs	Gravitational Waves
HBB	Hot Big Bang
ICT	Infinitesimal Coordinate Transformations
LSS	Last-scattering Surface
MD	Matter Dominated
RD	Radiation Dominated
SGWB	Stochastic Gravitational-wave Background
TT	Transverse-Traceless
ΛD	Λ Dominated

AKNOWLEDGEMENTS

I would like to thank two of my thesis advisers, Professor Nobuyuki Sakai and Associate Professor Ryo Saito, for their kind advice and continuous encouragement. Thanks also to Professor Kiyoshi Shiraishi and Dr Masashi Kuniyasu for their discussions on some exciting topics in cosmology. I am also grateful to Dr Mai Yashiki and all the Theoretical Astrophysics and Theoretical Sports Physics Laboratory members at Yamaguchi University for their help in carrying out the present work and daily life.

CHAPTER 1

Introduction

1.1 Searching for a Theory on the Origin of the Universe

"Where do we come from? What are we? Where are we going?" These deep age-old questions that vex humanity all the time are given in the title of a painting by Paul Gauguin (Figure 1.1.1). In a similar version, these questions are also asked by cosmologists: "How was the universe born? What is the universe made of? What will the universe be like in the future?" Remarkably, to some extent, these questions have reliable quantitative answers that have been tested against cosmological observations.

Two fundamental observational facts opened current modern cosmology. One fact is the expansion of the universe, which was first discovered by Edwin Hubble, who found that distant galaxies are receding from us with velocities increasing with distance [37]. The other fact is the homogeneous and isotropic of the universe on large scales ($\gtrsim 100\,\mathrm{Mpc}$). The large-scale homogeneity is supported by the uniform distribution of galaxies on scales larger than 300 million light years [88]. The strong evidence for isotropy is the highly isotropic distribution of thermal radiation at about $3\,\mathrm{K}$ which is permeating the universe [78]. This thermal radiation was first discovered by Arno Penzias and Robert Wilson in 1965 [63], and it is now called the cosmic microwave background (CMB).

Combining these two observational facts with the theory of general relativity, one obtained a paradigm called the standard Hot Big Bang (HBB) model, which

Fig. 1.1.1: The painting named *"Where Do We Come From? What Are We? Where Are We Going?"* by Paul Gauguin, 1897-98. This painting is download from the Museum of Fine Arts, Boston. [www.mfa.org]

successfully describes the universe's evolution from about 1 second after the beginning (if there is) to the present time. Figure 1.1.2 shows the brief thermal history of the universe based on the HBB model.

The standard HBB model is relatively simple and elegant and provides a testable account of the universe's history. No current observational evidence contradicts the Big Bang scenario. However, some shortcomings do exists. For example, the small temperature fluctuations in the CMB are coherent on a scale which is much larger than the largest possibly causal connected region [1]; this issue is often referred as the *horizon problem* of the HBB model. Although the universe is homogeneous and isotropic on large scales, it also has structures like clusters, galaxies, and stars on small scales. The HBB model can explain how these structures develop, but it cannot account for the *origin* of these structures. Most cosmologists now agree that all these mysteries may have a common explanation called the *inflation* [11, 36, 46, 74, 81].

Under the inflation scenario, the universe first undergoes an epoch of accelerated expansion dominated by vacuum energy. Then it enters several phases of decelerated expansion as depicted by the HBB model. Inflation solves the shortcomings of the HBB model by allowing the cosmological perturbations to be causally connected again at the beginning and by increasing the horizon's size in the early universe. In other

[1] The boundary of the largest causal connected region is often called the *horizon*.

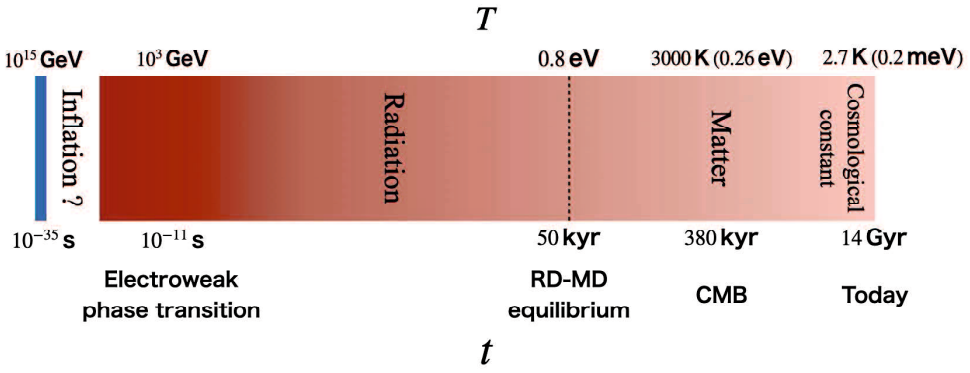

Fig. 1.1.2: A brief thermal history of the universe and several important moments. This figure refers to references [29, 54].

words, inflation provides a natural quantum-mechanical mechanism to explain the origin of the cosmological perturbations in the large structure of matter and in the CMB.

Unfortunately, since the energy scale associated with inflation is so large ($\sim 10^{13}$ TeV), it is very difficult to probe its physics experimentally. However, at least one signature of inflation is within reach of observations. The production of the primordial gravitational waves (GWs) is a crucial prediction of the inflationary scenario of the early universe [80, 32], since, during inflation, quantum fluctuations of the gravitational field would be generated simultaneously as those of other fields. However, unlike other non-gravitational fields that would eventually decay or transform as most inflation models suggest, fluctuations of gravitational field will be preserved and propagated to the present universe. Therefore, the signatures of primordial GWs, if observed, would give us the shape of the early universe that has not been seen yet.

1.2 Primordial Gravitational-Waves as a Probe of the Early Universe and the Purpose of this Thesis

Roughly speaking, there are two ways we can observe the primordial GWs: indirect and direct observations. A particular pattern of the CMB polarization called the $B-mode$ could be produced by primordial tensor perturbations (i.e. primordial GWs). These pattern cannot be mimicked by other space-time perturbations (like the scalar perturbations). Therefore, searching for the B-mode in CMB offers an indirect way of searching for the primordial GWs. In 2014, BICEP2 Collaboration once reported the detection of B-mode of CMB and claimed that it was due to the primordial GWs [6]. But later analysis found that the signal was due to the polarized interstellar dust [7].

The direct GW observations that began in 2015 [1, 2, 3] have opened up a new window to investigate various astrophysical phenomena which cannot be probed by conventional observations based on electromagnetic waves. Although the current terrestrial GW detectors are only sensitive to single, strong, and low-redshift GW events such as the merging of black holes, future detectors are expected to detect much weaker and high-redshift GW events or even the primordial GWs generated in the early universe. For example, the third-generation ground-based GW detector such as the Einstein Telescope and Cosmic Explore are expected to be able to detect GW events with redshift up to $z \approx 100$. Furthermore, the space-based detector Decihertz Interferometer Gravitational-Wave Observatory (DECIGO), with its primary target–searching the primordial GWs produced during inflation, is planned to launch a precursor observatory in the 2030s [75, 41]. Given these perspectives, it will be essential to study the methods of distinguishing primordial GWs from other GW signals.

In the present universe, the signal of primordial GWs is expected to be in the form of a stochastic gravitational-wave background (SGWB). SGWB is very different from

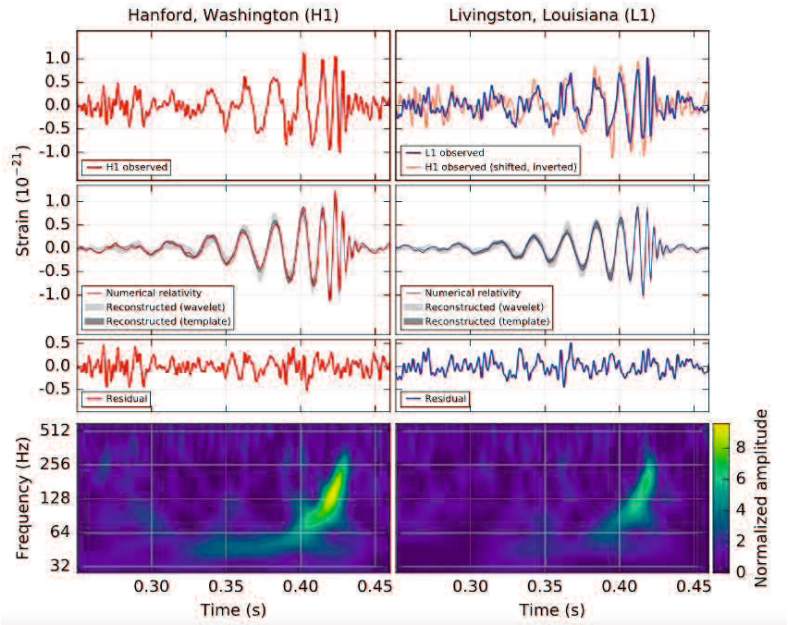

Fig. 1.2.1: The first observed GW event generated from a binary black hole merger. It has a specific waveform in the time domain and a flash in the time-frequency axis; these are not the case for an SGWB. This figure is from reference [2].

the signal of a single GW event generated by astrophysical objects, for example, the merger of binary black holes as shown in Figure 1.2.1. Because SGWBs do not possess a specific waveform, we can only characterize them by their energy densities, like those in Figure 1.2.2, which shows the expected energy densities of SGWB for different sources, the observational limits, and the sensitivities of GW detectors. Detection of the inflationary SGWB is difficult because its energy density is expected to be tiny. As we can see from Figure 1.2.2, in a typical frequency band of the GW detectors ($1 - 10^2\,\mathrm{Hz}$ for ground-based detector LIGO-Virgo or $10^{-3} - 1\,\mathrm{Hz}$ for space-based detector LISA), the expected energy density of SGWB in the slow-roll inflation (the blue line below) is much smaller than the energy density of typical astrophysical SGWB, like those generated by binary black holes or binary neutron stars (the purple and green lines in the middle).

Numerous studies have been carried out on the methods for separating the astrophysical components in SGWB, for example: spectral separation [82, 5, 62, 64, 20, 65], subtraction [67, 61, 76, 53, 70], anisotropies [9, 49, 18], and so on. These methods

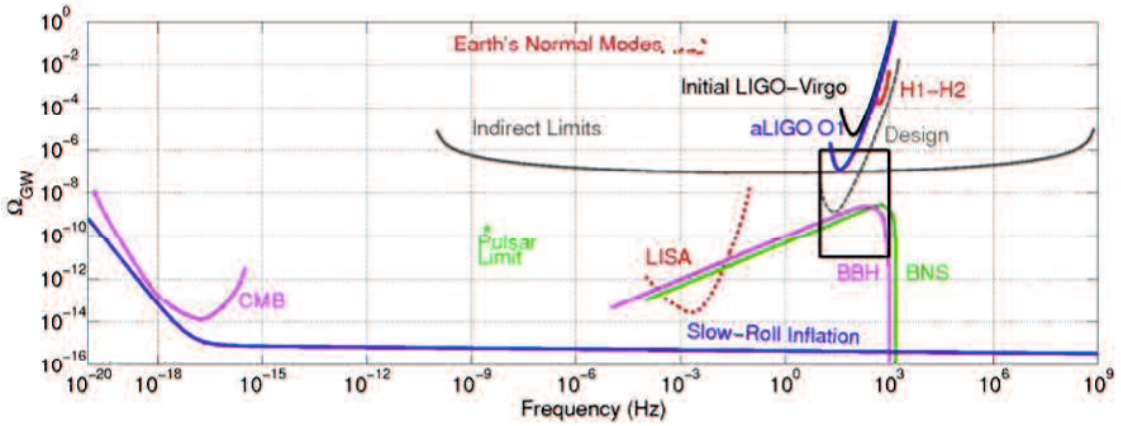

Fig. 1.2.2: Theoretical predictions of the energy density parameter $\Omega(f)$ for the SGWB of the slow-roll inflation and astrophysical sources, including Binary Black Holes (BBH) and Binary Neutron Stars (BNS). This figure also shows the detector's sensitivity (like LIGO-Virgo and LISA) and the observational bounds (like CMB) for the SGWB. This figure is from reference [4].

work well to place upper limits on the inflationary SGWB. However, in these methods, it is hard to guarantee that after subtraction, the remaining components are of the inflation origin without a priori assumption on an exact inflation model. For this reason, in this thesis, we investigate whether the inflationary SGWB is distinguishable from the other components of SGWB in direct observational experiments without any prior assumptions on the exact inflation model.

We focus on a unique and universal prediction of inflation: the generation of the super-horizon modes, modes with wavelengths larger than the horizon. Super-horizon modes could be generated during inflation but cannot be generated by any process in the post-inflationary universe. In consequence, the inflationary super-horizon modes of GWs have a standing-wave nature after the horizon re-entry [33, 35, 34, 26, 14]. The standing-wave nature is supposed to be observed as a unique property of the inflationary SGWB, that is, an angular correlation between GWs from the opposite directions. Although this property has already been noticed in the literature, we would like to emphasize it as a unique prediction of inflation and name it the *antipodal angular correlations (AAC)*. The astrophysical SGWB, on the other hand, will not have such type of angular correlations because individual astrophysical sources are

not correlated with each other.

About 20 years ago, Allen, Flanagan and Papa [14] showed that the above unique property of inflationary SGWB cannot be detected in the GW strain correlation analysis due to the finite frequency resolution in practical observations. Moreover, Margalit, Contaldi and Pieroni [51] recently pointed out that metric perturbations along the line-of-sight will randomize any phase information in the primordial GWs. The effect of metric perturbation will, of course, influence the detectability of the AAC. Taking into account the above two effects, in this thesis, we first investigate whether we can construct another estimator (such as the intensity) sensitive to the AAC. Since the analysis tells us that the unobservable of the AAC seems to be unavailable in practice, we then clarify the (un)observable angular correlations in the inflationary SGWB.

This thesis is organized as follows. In Chapter 2, we briefly review the HBB model and describe two main shortcomings in this model. In Chapter 3, after briefly reviewing its history, we introduce the inflation theory as a solution to the shortcomings of the HBB model; then, we present a simple model of inflation: the single field slow-roll inflation. In Chapter 4, we review the basic theory of GWs, focusing on the geometric description based on general relativity. We also derive the basic equation governing the evolution of GWs in cosmology and review the production of primordial GWs in inflation. Chapter 5 is devoted to the study of the AAC property in inflationary SGWB. We first review how to characterize an SGWB and then make a comprehensive deviation of the AAC property. After that, we analyze the detectability of AAC in both frequency and time domains. We conclude this thesis in Chapter 6.

1.3 Units and Notation

In most part of this thesis, we will use the natural units, i.e., the following fundamental constants are set to unity,

$$\hbar = c = k_B = 1\,. \tag{1.3.1}$$

We will depart form these natural units when concerning observations. In natural unit, all dimensions can be expressed in terms of the unit of energy, that is,

$$[\text{Length}]^{-1} = [\text{Time}]^{-1} = [\text{Mass}] = [\text{Temperature}] = [\text{Energy}] \ . \tag{1.3.2}$$

In this thesis, we shall follow the sign conventions of Minsner, Thorne and Wheeler [56]. In particular, we use the metric signature $(-,+,+,+)$. We use Greek letters to denote spacetime indices, and Latin letters from the middle of the alphabet $(i,j,...)$ to denote spatial indices. Spacetime indices are run through the values $0,1,2,3$; spatial indices are run through $1,2,3$.

CHAPTER 2

The Hot Big Bang (HBB) Model

2.1 The HBB Model of the Universe

Our present understanding of the evolution of the universe is based upon the standard Hot Big Bang (HBB) model of cosmology, or the Friedmann-Lemaître-Robertson-Walker (FLRW) cosmology model as another name. This model is based on two basic observational facts: the expansion of the universe and the large-scale homogeneity and isotropy. The expansion of the universe is based on Edwin Hubble's discovery in 1929 that the distant galaxies are receding from us with a velocity that increases with their distance [37]. A uniform distribution of galaxies on scales $\gtrsim 100\,\mathrm{Mpc}$ [28] tells us the universe is homogeneous on a large scale. The best evidence for the isotropy is the discovery of the cosmic microwave background (CMB) by Arno Penzias and Robert Wilson in 1965 [63] that shows a perfect blackbody spectrum in which the temperature fluctuations are only $|\delta T/T| \lesssim 3 \times 10^{-5}$.

A spatially homogeneous and isotropic universe can be described by the FLRW spacetime metric

$$ds^2 = -c^2dt^2 + a^2(t)\left[\frac{dr^2}{1-kr^2} + r^2d\theta^2 + r^2\sin^2\theta d\phi^2\right], \tag{2.1.1}$$

where $a(t)$ is called the scale factor and we say that the universe is expanding when $\dot{a} > 0$ or contracting when $\dot{a} < 0$ [1]. The sign of k represents the spatial curvature of the universe. This dissertation only considers the spatially flat ($k = 0$) case.

[1] In this thesis, we use a dot to represent the time derivative, i.e., $\dot{x} \equiv dx/dt$, $\ddot{x} \equiv d^2x/(dt)^2$.

On a large scale, the evolution of the scale factor $a(t)$ thus represents the evolution of the universe. The function $a(t)$ is determined by the Einstein equations

$$R_{\mu\nu} - \frac{1}{2} R\, g_{\mu\nu} = 8\pi G\, T_{\mu\nu}\,. \tag{2.1.2}$$

In a zeroth-order approximation, the energy-momentum tensor $T_{\mu\nu}$ must have the same symmetries of homogeneity and isotropy as the FLRW spacetime; therefore, it takes the form of a perfect fluid,

$$T^{\mu}_{\nu} = \mathrm{diag}\,(-\rho,\, p,\, p,\, p)\,, \tag{2.1.3}$$

where the energy density ρ and the pressure p are functions of time only.

Take the FLRW metric (2.1.1) and the energy-momentum tensor (2.1.3) into the Einstein equation; the time-time component yields the Friedmann equation

$$\left(\frac{\dot{a}}{a}\right)^2 = \frac{8\pi G}{3}\rho\,, \tag{2.1.4}$$

the spatial-spatial component yields

$$2\frac{d}{dt}\left(\frac{\dot{a}}{a}\right) + 3\left(\frac{\dot{a}}{a}\right)^2 = -8\pi G\, p\,. \tag{2.1.5}$$

The conservation of energy-momentum, $\nabla_\mu T^{\mu}_{\nu} = 0$, gives the equation

$$\dot{\rho} + 3\frac{\dot{a}}{a}(\rho + p) = 0\,. \tag{2.1.6}$$

Combining equation (2.1.5) and the Friedmann equation (2.1.4) results in the *acceleration* equation

$$\frac{\ddot{a}}{a} = -\frac{4\pi G}{3}(\rho + 3p)\,. \tag{2.1.7}$$

Only two of the above four equations are independent; which one to use depends on the situation.

To fully determine the evolution, we need one more equation. This can be given

by the equation of state of the cosmological fluid, $p(t) = w\rho(t)$, where w is called the equation-of-state parameter. For nonrelativistic particles ("matter"), $w = 0$; for relativistic particles ("radiation"), $w = 1/3$; for vacuum energy (or the cosmological constant Λ), $w = -1$. Plugging the equation of state into the Friedmann equation (2.1.4) and the equation (2.1.6), we obtain the evolution equations for each single fluid

$$\text{Matter}: \quad \rho \propto a^{-3},\ a \propto t^{2/3}\,; \tag{2.1.8}$$

$$\text{Radiation}: \quad \rho \propto a^{-4},\ a \propto t^{1/2}\,; \tag{2.1.9}$$

$$\text{Cosmological constant } \Lambda: \quad \rho = \frac{\Lambda}{8\pi G},\ a \propto e^{\sqrt{\frac{\Lambda}{3}}t}\,. \tag{2.1.10}$$

Observational data tells us that in the present epoch, the universe is dominated by a cosmological constant which accounts for nearly 70% of its total energy density [87], matter accounts for approximately 30% [8], while radiation accounts for less than 0.01%. Relations (2.1.8) and (2.1.9) tell us that as the scale factor $a(t)$ decreases toward the past, then matter would dominate the energy density of the universe for a while. Eventually, radiation would dominate at the beginning of the universe. Therefore, in the HBB model, the universe's rough history is separated into three parts: it starts from a radiation-dominated (RD) epoch, then turns into a matter-dominated (MD) epoch as the expansion, and reaches the present cosmological constant dominated epoch.

2.2 Shortcomings of the HBB Model

Before we carefully examine these shortcomings, let us first define some useful quantities in the discussion of cosmology.

If we write the FRLW metric (2.1.1) in a conformal form:

$$ds^2 = -a^2(t)(d\eta^2 - d\mathbf{x}^2)\,, \tag{2.2.1}$$

then the spatial coordinate $\mathbf{x}$ is called the *comoving distance*, and the time coordinate η is called the *conformal time*. The conformal time η is related to the (cosmic) time t by

$$d\eta = \frac{1}{a(t)} dt \,. \tag{2.2.2}$$

Since light travels along null curves on which $ds^2 = 0$, for photons, its conformal time is equal to its comoving distance. Therefore, the conformal time of photon defines the maximum radius of a region that can be causally connected. Such maximum causally connected radius is called the *(comoving) particle horizon*, or *(comoving) causal horizon*, and it is equal to the conformal time $\eta(t)$:

$$\eta(t) = \int_0^t \frac{dt'}{a(t')} \,. \tag{2.2.3}$$

Another scale that is frequently used to estimate the size of the universe is the *Hubble radius*, $H^{-1}(t)$. The function $H(t)$ is defined as the fractional rate of the increase of distances:

$$H(t) \equiv \left(\frac{da}{dt} \right) / a = \frac{\dot{a}}{a} \,, \tag{2.2.4}$$

and it is called the *Hubble parameter*. Since the physical distance from a nearby galaxy to us can be represented as $\mathbf{l} = a(t)\,\mathbf{x}$, the receding velocity of the galaxy is $\mathbf{v} \equiv d\mathbf{l}/dt = H(t) \cdot \mathbf{l}$. The Hubble radius H^{-1}, therefore, represents the time it would have taken for the galaxy to attain its present separation if it had maintained the present receding velocity all the time. Thus the Hubble radius also gives us an approximation of the *local* size of the universe. The *comoving Hubble radius*, $\mathcal{H}^{-1}$, is defined as

$$\mathcal{H}^{-1} \equiv \left(\frac{a'}{a} \right)^{-1} = \frac{1}{Ha} \,. \tag{2.2.5}$$

Now let us take a look at the shortcomings of the HBB model. The first one is the *large-scale smoothness*, or the *horizon problem* as it was usually called. The temperature fluctuation of CMB at the level of $\delta T/T \sim 10^{-5}$ tells us that the universe was very smooth when the CMB photons observed today decoupled from electrons and started to propagate freely at the age of about 3.8×10^5 years. This moment is

called the *decoupling* and it defines a hyper-surface named the *last-scattering surface (LSS)* in the space-time diagram (see Figure 2.2.1) [2]. The smoothness of the LSS implies that different points on it should have been causally connected before. In the space-time diagram, this means that the past light-cones for two arbitrary points are crossing (the situation of diagram (a) in Figure 2.2.1). We can see directly from the diagram that the cross of light-cones is equivalent to the condition $2\eta_{\rm LSS} \geq \eta_0$, where $\eta_{\rm LSS}$ and η_0 are the conformal times at decoupling and present, respectively. On the other hand, we can also calculate each conformal time in the HBB scenario by

$$\eta = \int_0^t \frac{dt'}{a(t')} = \int_0^a \frac{da'}{a'^2 H(a')}, \tag{2.2.6}$$

where we have changed the variable from t to the scale factor a. At each moment, the scale factor can be estimated from its relation with temperature $T \propto a^{-1}$ [3]. The temperature of the universe at decoupling is about 2000 K and at present is about 2.7 K. However, numerical calculations [4] show that the conformal time at the LSS is only about $\eta_{\rm LSS}/\eta_0 \simeq 0.02$, comparing with the current conformal time η_0. This is to say that there are points on the LSS for which their past light-cones do *not* overlap (the situation (b) in Figure 2.2.1). Thus, these points have not ever been causally connected before. Nevertheless, all the points on LSS indeed have a uniform temperature to within one part in 10^5 according to the CMB observation, and this is quite unnatural.

The second one is the *small-scale inhomogeneity*, or called the *initial perturbation problem*. While the universe is very smooth on large scales, it also has abundant structures such as stars, galaxies, and clusters on scales smaller than 100 Mpc. The seeds of these structures should be the initial perturbations in the early universe. However, the HBB model can explain only the formation of these structures by the growth of initial perturbations through gravitational instability; it has trouble explaining the generation of the initial perturbations.

[2] Before decoupling, photons were kept in equilibrium with electrons by Compton scattering (see, for example, [86] with a detailed description of the thermal history of the universe).

[3] See, for example, section 5.4 in [83] for the deviation.

[4] For example, section 17.6.5 in [48].

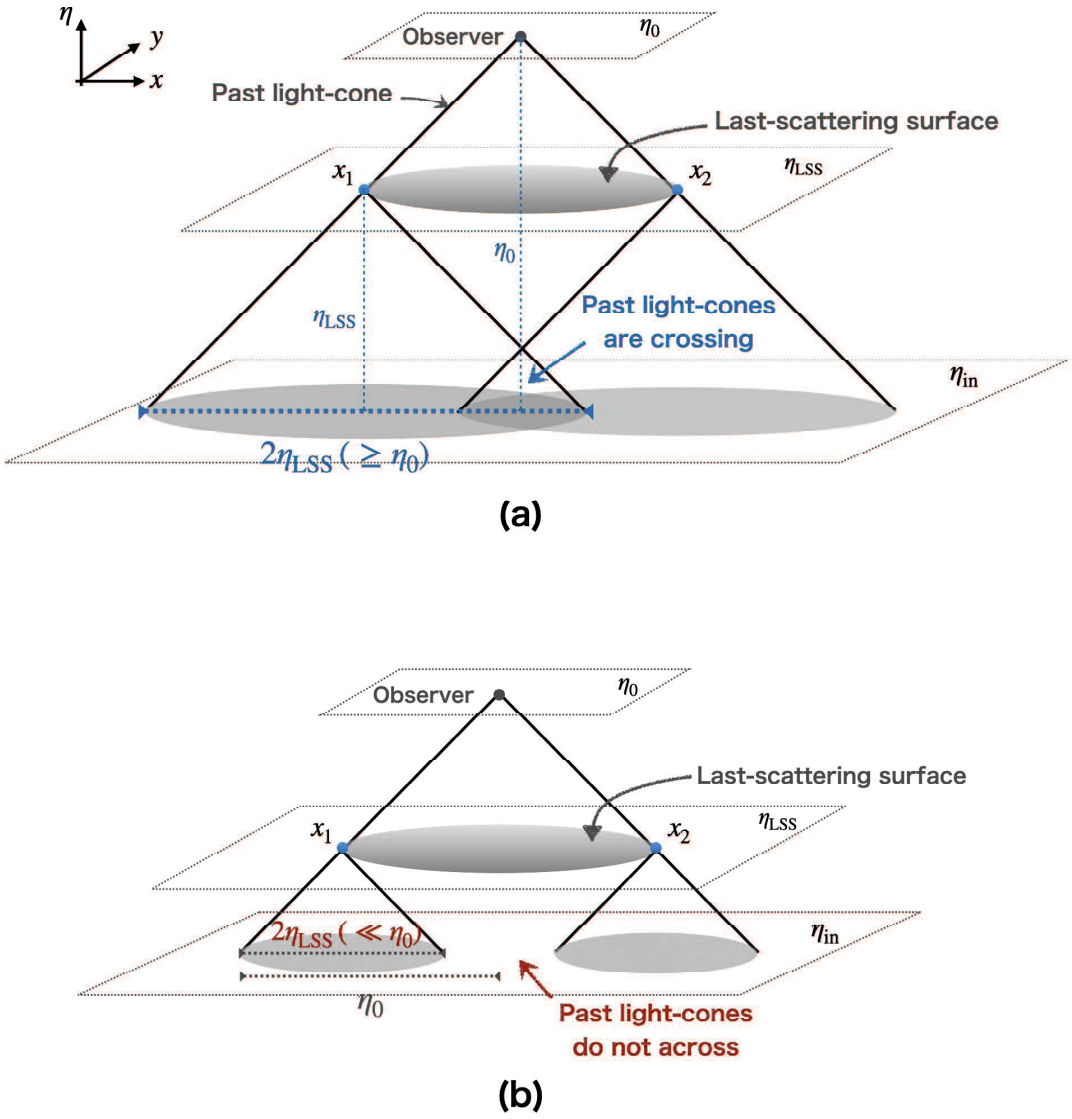

Fig. 2.2.1: An illustration of the horizon problem in the spacetime diagram. The solid diagonal lines represent past light-cones for each spacetime point where the light signals came in. All the causal processes that can influence each spacetime point are within its past light-cone. According to the CMB observation, two arbitrary points x_1 and x_2 on the LSS have almost the same temperature, which implies that their past light-cones should be crossing (the situation of diagram (a)). However, in the HBB model, calculation shows that $2\eta_{\rm LSS} \ll \eta_0$ (the situation of diagram (b)). This means that the past light-cones for these two points do not cross, and they have never been causally connected.

Suppose a perturbation at present has the proper wavelength (i.e. physical wavelength) $\lambda_0 \equiv \lambda(t_0)$. This wavelength can be associated with an invariant quantity $M(\lambda)$ that represents an amount of non-relativistic mass contained inside of a sphere of radius $\lambda/2$ [60]:

$$M(\lambda) = \frac{4\pi}{3}\left(\frac{\lambda}{2}\right)^3 \rho_{\text{n.r.}}\,, \tag{2.2.7}$$

where $\rho_{\text{n.r.}}$ is the energy density of the non-relativistic mass. For a typical galaxy with mass $M \sim 10^{11}\,\text{M}_\odot$, where $\text{M}_\odot$ is the mass of the Sun, the present proper wavelength of perturbation λ_0 is about 1 Mpc [60]. Now the proper wavelength would evolves as $\lambda(t) = a(t)\lambda_0 \propto t^n$ if we assume $a(t) \propto t^n$. On the other hand, the Hubble radius H^{-1} evolves as $H^{-1} = n^{-1}t$. Then the ratio between the proper wavelength and the Hubble radius follows $\lambda/H^{-1} \propto n \cdot t^{n-1}$. In the Big Bang model $n < 1$ in the initial and matter-dominated phase. The above relation means that the wavelength of perturbations smaller than the Hubble radius today will be larger than the Hubble radius in the past as $t \to 0$. However, normally physical processes can only have influence over a scale smaller than the Hubble radius. It is unnatural that the relevant astrophysical perturbations are much larger than the Hubble radius in the past.

The horizon and initial perturbation problems are not the only shortcomings that the HBB model suffers from. There are also the flatness and the monopole problems [87], but the two problems we have just introduced are more serious than the others.

CHAPTER 3

Inflation Theory

3.1 Brief History of the Inflation Theory

The idea of an early possible exponential expansion was proposed by several authors in the late 1970s, and early 80s [81, 42, 74, 59]. However, it was Alan Guth [36] who gave a clear physical motivation to introduce an exponential expansion phase in the early universe. Guth's model, now called the "old inflation," assumes a scalar field initially trapped in a false vacuum state due to a supercooling of the initial hot universe. The energy of the universe would remain constant for a while and thus provide an exponential expansion. The inflation would be stopped by the quantum barrier penetration effect in which the scalar field penetrates to a true vacuum state (see the potential (a) in Figure 3.1.1). The scalar field would then oscillates around the true vacuum state, and the universe would translate into the radiation-dominated phase. However, this intuitive picture did not work because the inflation produced was too short to solve any problems [87, 60].

Guth's model was soon replaced by a version proposed by Linde [46] and by Albrecht, and Steinhardt [11], known as the "new inflation". This version is based on the Coleman-Weinberg [25] type potential (the potential function (b) in Figure 3.1.1). This potential function is very flat around $\phi = 0$. The inflation may begin with $V(\phi = 0)$. This state is unstable due to quantum fluctuations, and the scalar field would slowly roll towards the global minimum of the potential. The inflation ends with the scalar field oscillating around the global minimum. The key difference between the new and old inflation scenario is that for the new scenario $\dot{\phi} \neq 0$ and thus could

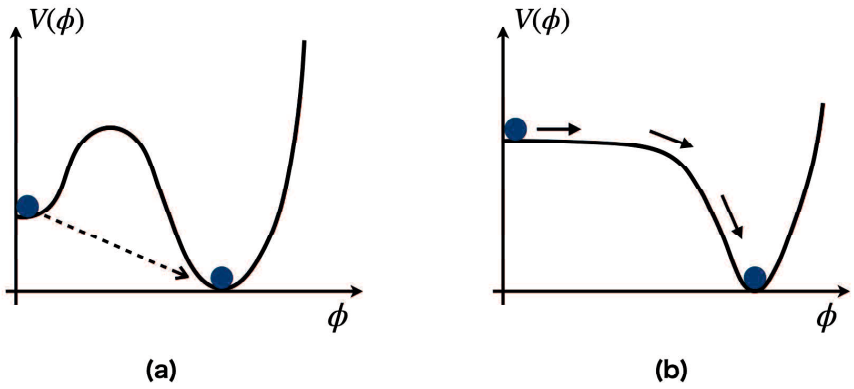

Fig. 3.1.1: Two models of the potential function for inflation.

ensure sufficient inflation to make the universe homogeneous [45]. Unfortunately, the new inflation model requires the potential of the scalar field ϕ to have a quite flat plateau near $\phi = 0$, which is quite unlikely in a pre-inflationary state of the universe.

So far, more than hundreds of different inflation models have been proposed [52], but no single model can be considered entirely satisfactory. Of course, in the lack of the underlying fundamental physics in the early universe, one is free to play with potential and invent more new models. Nevertheless, inflation as a plausible theory is not due to the number of models it allows but because it can solve the HBB model's problems and explain the origin of the universe's large-scale structure. Let us see how inflation could do this.

3.2 Inflation as a Solution to the Shortcomings of the HBB model

In section 2.2 we have shown two problems of the HBB model; in this section, we explain how inflation, i.e., an accelerated expansion epoch before the radiation-dominated period, could solve these problems.

3.2.1 Solution to the Horizon Problem

The cause of the horizon problem is that the comoving particle horizon (i.e., the conformal time) at the LSS, $\eta_{\rm LSS}$, is too small compared with the present comoving particle horizon η_0. This problem can be solved by introducing an accelerating expansion period before the RD to increase the (comoving) particle horizon in the early universe. As in equation (2.2.6), we can change the integral variable for the conformal time into the scalar factor, that is

$$\eta = \int_0^t \frac{dt'}{a(t')} = \int_0^a \frac{1}{Ha} d(\ln a) = \int_0^a \mathcal{H}^{-1} d(\ln a)\,, \tag{3.2.1}$$

where $\mathcal{H}^{-1}$ is the comoving Hubble radius defined in (2.2.5). In the HBB model, because $\mathcal{H}^{-1}$ is always an increasing function ($\mathcal{H}^{-1} \propto a$ for the RD epoch and $\mathcal{H}^{-1} \propto a^{1/2}$ for the MD epoch), the main contribution to η must comes from late-times. To "gain" sufficient causal distance $\eta_{\rm LSS}$ to solve the horizon problem, one reasonable way is to make $\mathcal{H}^{-1}$ decrease for a while in the early times; this is equal to

$$\mathcal{H}^{-1} \equiv (\dot{a})^{-1} \text{ is decreasing} \Leftrightarrow \dot{a} \text{ is increasing} \Leftrightarrow \ddot{a} > 0\,. \tag{3.2.2}$$

Therefore, an accelerating expansion period can solve the horizon problem.

3.2.2 Explaining the Origin of Perturbations

The problem with generating initial perturbations is that in the initial time, perturbations' wavelengths are large the Hubble radius. A natural solution to this problem is to again make the wavelength smaller than the Hubble radius in the early times, $\lambda < H^{-1}$ when $t \sim 0$. If this condition is satisfied, physical processes can lead to initial perturbations. Now consider an exponential expansion period with $a(t) \propto e^{H_{\rm inf.} t}$ before the RD phase, where $H_{\rm inf.}$ is the Hubble parameter during inflation and we assume it is nearly a constant. Then the evolution of the Hubble radius $H^{-1} = a/\dot{a}$

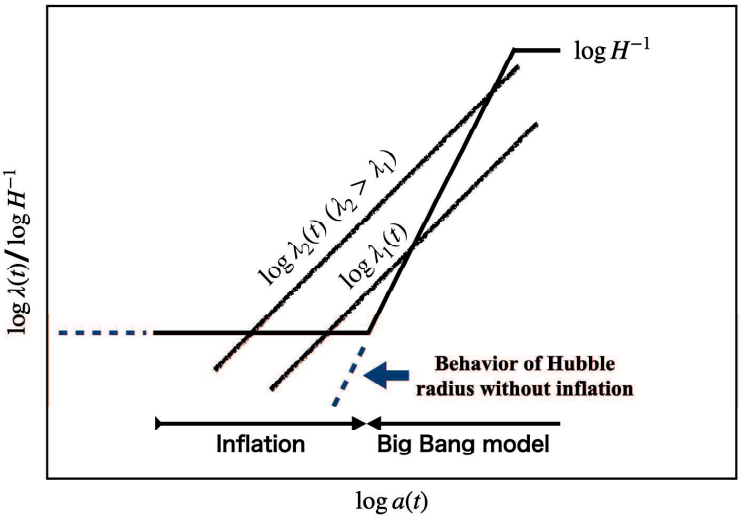

Fig. 3.2.1: The evolution of the Hubble radius H^{-1} and the physical wavelength of perturbation. Note that the horizontal axis is taken to be $\log a(t)$ so the wavelength evolves as a straight line.

after adding an inflation phase becomes:

$$H_{\text{inf.}}^{-1} = \text{const. (inflation)} \longrightarrow 2t \text{ (RD)} \longrightarrow \frac{3t}{2} \text{ (MD)} \longrightarrow H_{\Lambda}^{-1} = \text{const. } (\Lambda\text{D})\,. \tag{3.2.3}$$

On the other hand, the wavelength of perturbation, $\lambda(t) = \frac{\lambda_0}{a(t_0)} a(t)$, evolves as the same as the scale factor:

$$\lambda_0 e^{tH_{\text{inf.}}} \text{ (inflation)} \longrightarrow \lambda_0 t^{1/2} \text{ (RD)} \longrightarrow \lambda_0 t^{2/3} \text{ (MD)} \longrightarrow \lambda_0 e^{H_\Lambda} \text{ } (\Lambda\text{D})\,. \tag{3.2.4}$$

Plotting the evolution of H^{-1} and λ into the Fig. 3.2.1, we see that after introducing an inflation period, the wavelength of perturbation can be smaller than the Hubble radius at both the initial and the present epoch. This condition is possible because, during inflation, the Hubble radius remains constant while the wavelength increases exponentially.

3.3 A Simple Model of Inflation: Single Field Slow-Roll Inflation

The above section shows how inflation could solve two shortcomings of the Big Bang model. In this section, we introduce an exact and perhaps the simplest inflation model: called the *single field slow-roll inflation*.

Since inflation means an accelerating expansion, that is, $\ddot{a} > 0$, according to the acceleration equation (2.1.7), this corresponding to

$$p < -\frac{1}{3}\rho\,. \tag{3.3.1}$$

In other words, inflation means *a period dominated by a component with the equation-of-state parameter* $w < 1/3$.

To satisfy the above condition, a simple choice is a positive cosmological constant $\Lambda_{\text{inf.}}$[1] which posses an energy density $\rho = \Lambda_{\text{inf.}}/(8\pi G)$ and a pressure $p = -\Lambda_{\text{inf.}}/(8\pi G)$, that is, $w = -1$. From the Friedman equation (equation (2.1.4) in Chapter 1),

$$H^2 = \frac{8\pi G}{3}\rho = \frac{\Lambda_{\text{inf.}}}{3} = \text{Const.}\,, \tag{3.3.2}$$

we see the Hubble parameter is a constant, and we denote it by $H = H_{\text{inf.}}$. The scale factor evolves as $a(t) \propto e^{H_{\text{inf.}}t}$.

To mimic this cosmological constant, let us consider a scalar field $\phi(\mathbf{x}, t)$ assigned to each spacetime point. The scalar field has the dimension of energy, ϕ[eV], and it is associated with a potential energy $V(\phi)$. We shall call this scalar field the "inflaton field", and suppose that the universe only contains this inflaton field plus a flat FLRW metric in the inflation period. Now let us consider under what conditions this scalar field could behave like a cosmological constant.

[1] This cosmological constant is different from the cosmological constant responsible for the current accelerating expansion.

The action for the inflaton field is the usual action of a scalar field:

$$S_\phi = \int d^4x\sqrt{-g}\left[-\frac{1}{2}g^{\mu\nu}\partial_\mu\phi\partial_\nu\phi - V(\phi)\right], \tag{3.3.3}$$

where g represents the determinant of the metric $g_{\mu\nu}$. The energy-momentum tensor of the inflaton field can be found by

$$T_{\mu\nu} \equiv -\frac{2}{\sqrt{-g}}\frac{\delta S_\phi}{\delta g^{\mu\nu}}. \tag{3.3.4}$$

With the help of the relation $\delta\sqrt{-g} = (-1/2)\sqrt{-g}\, g_{\mu\nu}\, \delta g^{\mu\nu}$, we could obtain

$$T_{\mu\nu} = \partial_\mu\phi\partial_\nu\phi - g_{\mu\nu}\left[\frac{1}{2}\partial^\mu\phi\partial_\nu\phi + V(\phi)\right]. \tag{3.3.5}$$

Take the flat FLRW metric (equation (2.1.1) in Chapter 1) into the above relation, suppose the inflaton field is also spatially homogeneous, that is, $\phi(\mathbf{x}, t) = \phi(t)$, we can read the energy density and the pressure of the inflaton field as follows

$$\rho_{\text{inf.}} = \frac{1}{2}(\dot{\phi})^2 + V(\phi), \tag{3.3.6}$$

$$p_{\text{inf.}} = \frac{1}{2}(\dot{\phi})^2 - V(\phi). \tag{3.3.7}$$

We see that if

$$\frac{1}{2}(\dot{\phi})^2 \ll V(\phi), \tag{3.3.8}$$

then

$$\rho_{\text{inf.}} \approx -p_{\text{inf.}} \approx V(\phi), \tag{3.3.9}$$

that is, if the scalar field changes very slowly as a function of time, then it could behave like a cosmological constant $\Lambda_{\text{inf.}}$. The condition (3.3.8) is often called the *first slow-roll condition*.

If condition (3.3.8) is satisfied, we also require that this condition be maintained over an extended period to solve the problems in the Big Bang model. This requirement can be satisfied by imposing that the absolute value of the time derivative of

the left-hand side of condition (3.3.8) should be much smaller than the absolute value of the time derivative of the right-hand side; this will leads to

$$|\ddot{\phi}| \ll |dV/(d\phi)|\,, \tag{3.3.10}$$

which is called the *second slow-roll condition*.

In this scalar-field-dominated period, the Friedmann equation and the energy-momentum conservation equation are:

$$H^2 = \frac{8\pi G}{3}\rho_{\text{inf.}}\,, \tag{3.3.11}$$

$$\dot{\rho}_{\text{inf.}} + 3H(\rho_{\text{inf.}} + p_{\text{inf.}}) = 0\,. \tag{3.3.12}$$

Taking the energy density (3.3.6) and the pressure (3.3.7) into equation (3.3.12), we obtain an equation that governing *the evolution of the scalar field*:

$$\ddot{\phi} + 3H\dot{\phi} = -\frac{dV}{d\phi}\,. \tag{3.3.13}$$

This equation mimics the equation of motion of a particle; $-dV/(d\phi)$ acting like an accelerating force, the expansion of the universe acting like a friction term which slows the "movement" of the inflaton field toward the point of minimum potential.

Take time derivative of equation (3.3.11) and using equation (3.3.12), we obtain a useful relation

$$\dot{H} = -4\pi G(\dot{\phi})^2\,. \tag{3.3.14}$$

According to the first slow-roll condition (3.3.8), equation (3.3.11) becomes

$$H^2 \approx \frac{8\pi G}{3}V(\phi)\,. \tag{3.3.15}$$

Combining the first slow-roll condition (3.3.8), equation (3.3.14), and equation (3.3.15), we obtain

$$-\dot{H} \ll 3H^2\,, \tag{3.3.16}$$

that is to say, *the Hubble parameter H changes very slowly over the time scale H^{-1}*.

In summary, a homogeneous scalar field $\phi(t)$ associated with a potential energy $V(\phi)$ can act like a cosmological constant and triggers inflation; on the condition that the scalar field changes very slowly as a function of time, and its potential is very large to dominated the energy density of the universe. To ensure the inflation lasts for an extended period, the second slow-roll condition (3.3.10) should be satisfied. The evolution of the scalar field is governed by equation (3.3.13), and during inflation, the Hubble constant H remains almost constant.

CHAPTER 4

Theory of Gravitational Waves (GWs)

4.1 Two Different Languages for Describing GWs

There are two different languages that we could use to describe gravitational waves. One is the *geometric language of general relativity*, in which the metric of spacetime $g_{\mu\nu}$ can be divided into

$$g_{\mu\nu} = \bar{g}_{\mu\nu} + h_{\mu\nu}\,, \quad |h_{\mu\nu}| \ll 1\,, \tag{4.1.1}$$

where $\bar{g}_{\mu\nu}$ is the background spacetime that could be the FLRW geometry, and gravitational waves, $h_{\mu\nu}$, are interpreted as the perturbations in the spacetime geometry. The other language is the classical or even quantum *field-theoretical language*, in which we do not interpret $h_{\mu\nu}$ as a spacetime metric but as a spin-2 massless field living in flat spacetime with the Minkowski metric $\bar{g}_{\mu\nu} = \eta_{\mu\nu}$, governed by the Fierz-Pauli action [31, 47]:

$$S = \frac{1}{2}\int d^4x\,(-\partial_\alpha h_{\mu\nu}\partial^\alpha h^{\mu\nu} + 2\partial_\alpha h_{\mu\nu}\partial^\nu h^{\mu\alpha} - 2\partial_\nu h^{\mu\nu}\partial_\mu h + \partial^\mu h\partial_\mu h)\,, \tag{4.1.2}$$

where $h \equiv \eta^{\mu\nu}h_{\mu\nu}$.

Both languages have their advantages. The geometric language is very suitable for describing the propagation of gravitational waves in a background spacetime, the interaction of gravitational waves with detectors, and all the astrophysical mechanisms

of gravitational wave production. On the other hand, the field-theoretical language is convenient for describing the energy and momentum carried by gravitational waves or the cosmological gravitational wave production mechanism. Both languages are descriptions of the linearized theory of gravity, but they are from different perspectives. One is from the geometric perspective of general relativity, the other from the quantum field theory perspective. Which one to be used depends on the situation. Since the subject of this thesis is the observation of primordial GWs, we will use the geometrical language most of the time, except in the discussion of the production of primordial GWs. Let us review the geometric description of GWs.

4.2 Geometrical Description of GWs

The geometric point of view for gravity is the viewpoint taken by general relativity. The concept of gravitational waves merges from a weak-field approximation to Einstein's equations.

Consider the weak-field situation

$$g_{\mu\nu} = \eta_{\mu\nu} + h_{\mu\nu}\,, \quad |h_{\mu\nu}| \ll 1\,, \tag{4.2.1}$$

and we want to expand Einstein's equation to linear order in $h_{\mu\nu}$. For the convenience of discussion, we assume the background is a flat spacetime with the Minkowski metric $\eta_{\mu\nu}$.

The calculation is straightforward; only remember that since one expands in powers of $h_{\mu\nu}$, indices are raised and lowered using $\eta_{\mu\nu}$ and $\eta^{\mu\nu}$. To linear order, the Riemann tensor becomes

$$R_{\alpha\mu\beta\nu} = \frac{1}{2}(\partial_\mu\partial_\beta h_{\alpha\nu} + \partial_\alpha\partial_\nu h_{\mu\beta} - \partial_\mu\partial_\nu h_{\alpha\beta} - \partial_\alpha\partial_\beta h_{\mu\nu})\,. \tag{4.2.2}$$

The Ricci tensor $R_{\mu\nu} \equiv g^{\alpha\beta}R_{\alpha\mu\beta\nu} \approx \eta^{\alpha\beta}R_{\alpha\mu\beta\nu}$ becomes

$$R_{\mu\nu} = \frac{1}{2}(\partial^\alpha\partial_\nu h_{\mu\alpha} + \partial^\alpha\partial_\mu h_{\nu\alpha} - \partial^\alpha\partial_\alpha h_{\mu\nu} - \partial_\mu\partial_\nu h)\,, \tag{4.2.3}$$

where h is also defined by $h =\equiv \eta^{\alpha\beta}h_{\alpha\beta}$. The curvature scalar $R \equiv g^{\mu\nu}R_{\mu\nu} \approx \eta^{\mu\nu}R_{\mu\nu}$ becomes

$$R = \partial^\mu\partial^\nu h_{\mu\nu} - \partial^\alpha\partial_\alpha h\,. \tag{4.2.4}$$

Finally, in linear approximation, the Einstein equation $R_{\mu\nu} - (1/2)Rg_{\mu\nu} = 8\pi G T_{\mu\nu}$ becomes

$$\partial_\mu\partial^\alpha\bar{h}_{\nu\alpha} + \partial_\nu\partial^\alpha\bar{h}_{\mu\alpha} - \partial_\alpha\partial^\alpha\bar{h}_{\mu\nu} - \eta_{\mu\nu}\partial^\alpha\partial^\beta\bar{h}_{\alpha\beta} = 16\pi G T_{\mu\nu}\,, \tag{4.2.5}$$

here we define the "bar" operator as any symmetric tensor by

$$\bar{h}_{\mu\nu} \equiv h_{\mu\nu} - \frac{1}{2}\eta_{\mu\nu}h\,, \tag{4.2.6}$$

and to write the field equation in the above form we also used the relation $\bar{\bar{h}}_{\mu\nu} = h_{\mu\nu}$. Equation (4.2.5) is called the *linearized field equations* [56].

4.2.1 Lorentz Gauge

In the linearized field equations, the ten components (4.2.5) are not all independent. In fact, we could choose a specific coordinate in which the following conditions are satisfied

$$\partial^\nu\bar{h}_{\mu\nu} = 0\,, \tag{4.2.7}$$

Under the above conditions, the linearized field equations (4.2.5) become a simple form

$$\Box\bar{h}_{\mu\nu} = -16\pi G T_{\mu\nu}\,, \tag{4.2.8}$$

where $\Box = \partial_\alpha\partial^\alpha$ is the d'Alembertian operator. Condition (4.2.7) is called the *Lorentz gauge condition*. The choice of a particular coordinate is often called *fixing the gauge*.

The reason why we can impose the Lorentz gauge condition on the field equation is as follows. First, let us consider an *infinitesimal coordinate transformations (ICT)*

$$x^\mu \mapsto x'^\mu = x^\mu + \xi^\mu\,, \tag{4.2.9}$$

where ξ^μ are four arbitrary functions and we require that there derivatives $|\partial_\mu \xi_\nu|$ are not larger than $|h_{\mu\nu}|$. Then, under this ICT, the metric perturbations transform as

$$h_{\mu\nu} \mapsto h'_{\mu\nu} = h_{\mu\nu} - \partial_\mu \xi_\nu - \partial_\nu \xi_\mu \,. \tag{4.2.10}$$

Using the above relation, we can check that the Riemann tensor (4.2.2) is invariant under the transformation of (4.2.9); that is

$$R'_{\alpha\mu\beta\nu} = R_{\alpha\mu\beta\nu} \,. \tag{4.2.11}$$

Therefore, linearized field equations (4.2.5) are also *invariant* under the ICT.

Then we can use this freedom in the choice of coordinates to require that $\partial_\alpha \bar{h}'^{\alpha\mu} = 0$ in a new coordinate system; this requirement is equal to choosing ξ^μ so that

$$\Box \xi^\mu = \partial_\alpha h^{\alpha\mu} \,. \tag{4.2.12}$$

Because the d'Alembertian operator is invertible, equation (4.2.12) always has a solution. Therefore, we can always find a coordinate system that satisfies the Lorentz gauge condition (4.2.7).

4.2.2 Plane Wave Solutions and the Transverse Traceless Gauge

In the case of vacuum, the linearized field equation (4.2.8) under the Lorentz gauge reduces to the familiar wave equations

$$\Box \bar{h}_{\mu\nu} \equiv \partial_\alpha \partial^\alpha \bar{h}_{\mu\nu} = 0 \,. \tag{4.2.13}$$

Solutions for these wave equations are propagating gravitational perturbations called *gravitational waves (GWs)*.

The simplest solution to (4.2.13) is the monochromatic plane wave solution

$$\bar{h}_{\mu\nu}(\mathbf{x}, t) = \mathrm{Re}\left\{ A_{\mu\nu} e^{i k_\alpha x^\alpha} \right\} \,, \tag{4.2.14}$$

where $k_\alpha x^\alpha = -k_0 t + \mathbf{k}\cdot\mathbf{x}$, and Re{...} means take the real part inside the bracket. The amplitude $A_{\mu\nu}$ and the wave vector k_α are constants. Take (4.2.14) into (4.2.13) and (4.2.7), one obtain the following relations:

$$k_0{}^2 = |\mathbf{k}|^2 \Leftrightarrow k_\alpha k^\alpha = 0\,, \tag{4.2.15}$$

$$k^\mu A_{\mu\nu} = 0\,; \tag{4.2.16}$$

the first relation means that k^μ is a *null vector*; the second means that the wave vector k_μ is *orthogonal* to the amplitude $A_{\mu\nu}$.

However, not all of the six (ten minus four fixed by Lorentz gauge) degrees of freedom (DOF) in $\bar{h}_{\mu\nu}$ are physical DOF. In fact, there are only two physical DOF in the propagating wave solution (4.2.14), and the other four are residual gauge freedom. This fact can be seen as follows.

Suppose the spacetime perturbations $h_{\mu\nu}$ have already under the Lorentz gauge, that is $\partial^\mu \bar{h}_{\mu\nu} = \partial^\mu(h_{\mu\nu} - \frac{1}{2}h\eta_{\mu\nu}) = 0$. Then if we perform a further ICT of (4.2.9), the metric perturbations of course would transform like (4.2.10). However, the transformed perturbations $h'_{\mu\nu}$ could *still* be in the Lorentz gauge, i.e., $\partial^\mu \bar{h}'_{\mu\nu} = 0$, as long as we require $\Box\xi_\mu = 0$ for the infinitesimal transformation parameter. Since $\Box\xi_\mu = 0$ always have solutions, we could always make this coordinate transformation under the Lorentz gauge. Subtracting these four residual gauge freedom, we are left only two physical degrees of freedom in $\bar{h}_{\mu\nu}$.

We can show that [1] after some specific coordinate transformations, the metric perturbations $h_{\mu\nu}$ in (4.2.14) satisfy the conditions

$$h_{\mu 0} = 0\,, \quad h^k{}_k = 0\,, \quad \partial^j h_{ij} = 0\,. \tag{4.2.17}$$

These conditions define the *transverse-traceless gauge*, or TT gauge. Note that, since $h = h^\mu_\mu = 0$, there is no difference between $\bar{h}_{\mu\nu}$ and $h_{\mu\nu}$ in TT gauge.

Consider a monochromatic plane wave propagating in the z direction. In the TT

[1] See, for example, Section 18.1 in reference [48].

gauge, the constraints $h^{\rm TT}_{\mu 0} = 0$, $\partial^j h^{\rm TT}_{ij} = 0$, and $h^{{\rm TT}\,k}_{\ \ k}$ reveal that the only non-vanishing components of $h_{\mu\nu}$ are $h^{\rm TT}_{xx}$, $h^{\rm TT}_{yy}$, $h^{\rm TT}_{xy}$ and $h^{\rm TT}_{yx}$ which satisfy the relations

$$h^{\rm TT}_{xx} = -h^{\rm TT}_{yy} = {\rm Re}\left\{A_+ e^{ik(-t+z)}\right\}\,, \tag{4.2.18}$$

$$h^{\rm TT}_{xy} = h^{\rm TT}_{yx} = {\rm Re}\left\{A_\times e^{ik(-t+z)}\right\}\,, \tag{4.2.19}$$

where A_+ and $A_\times$ represent two independent amplitudes. Introducing two *polarization tensors* defined as

$$e^+_{\mu\nu}(\hat{\mathbf{z}}) = \begin{pmatrix} 0 & 0 & 0 & 0 \\ 0 & 1 & 0 & 0 \\ 0 & 0 & -1 & 0 \\ 0 & 0 & 0 & 0 \end{pmatrix}\,, \quad e^\times_{\mu\nu}(\hat{\mathbf{z}}) = \begin{pmatrix} 0 & 0 & 0 & 0 \\ 0 & 0 & 1 & 0 \\ 0 & 1 & 0 & 0 \\ 0 & 0 & 0 & 0 \end{pmatrix}\,. \tag{4.2.20}$$

A monochromatic plane wave propagating in the z direction in the TT gauge can be written as

$$h^{\rm TT}_{\mu\nu}(z,t) = {\rm Re}\left\{A_P\, e^P_{\mu\nu}(\hat{\mathbf{z}})\, e^{ik(-t+z)}\right\}\,, \tag{4.2.21}$$

where $P = +, \times$ represent two different polarization states.

Any gravitational waves can be resolved into a superposition of plane waves. We can introduce the transverse-traceless gauge of (4.2.17) for each plane wave in the superposition. Since these conditions are all linear in $h_{\mu\nu}$, we conclude that *for arbitrary gravitational wave, one can find a special coordinate frame in which* $h_{\mu\nu}$ *satisfies the constraints of* (4.2.17), that is

$$h_{\mu\nu} \mapsto h^{\rm TT}_{\mu\nu} \quad \text{(for arbitrary GW)}\,. \tag{4.2.22}$$

4.3 Cosmological GWs

In the last section, we have seen that the concept of gravitational waves is just two propagating physical degrees of freedom among the metric perturbations. In this section, we make a complete classification of the metric perturbations. Since the subject of this thesis is the primordial GWs generated in inflation, we will derive the equations governing the tensor perturbations. The background of perturbations is assumed to be the FLRW spacetime instead of the flat spacetime of Minkowski.

Most of the derivations in this section refers to references Dodelson and Schmidt [29], Maggiore [48] and Matsubara [55]. Two classical review articles on cosmological perturbation theory are Kodama and Sasaki [44] and Mukhanov, Feldman and Brandenberger [58].

4.3.1 Scalar-vector-tensor Decomposition of Metric Perturbations

Let us consider an FLRW spacetime with small metric perturbations. For the convenience of discussion, we shall use the conformal time η, and the comoving spatial coordinates $\mathbf{x}$ as the coordinates $x^\mu = (\eta, \mathbf{x})$, and write the FLRW background as

$$ds^2 = a^2(\eta)\left(-d\eta^2 + d\mathbf{x}^2\right) = a^2(\eta) \cdot \eta_{\mu\nu} dx^\mu dx^\nu \,. \tag{4.3.1}$$

Then the spacetime with perturbations $h_{\mu\nu}(\eta, \mathbf{x})$ can be written as

$$ds^2 = a^2(\eta)(\eta_{\mu\nu} + h_{\mu\nu}) dx^\mu dx^\nu \,. \tag{4.3.2}$$

Next, we decompose the ten independent components of $h_{\mu\nu}$ via their behaviour under spatial rotations. Because the time-time component h_{00} is invariant under spatial rotations, it is a 3-scalar, and we write it as

$$h_{00} = 2A \,, \tag{4.3.3}$$

where $A(\eta, \mathbf{x})$ is a scalar field.

The time-space component h_{0i} transforms as a spatial vector under rotations thus, it is a 3-vector, and we decompose it into a longitudinal part and a transverse part by a scalar field B and a vector field E_i:

$$h_{0i} = \partial_i B + E_i \,, \tag{4.3.4}$$

where E_i satisfies the constraint

$$\partial^i E_i = 0 \,. \tag{4.3.5}$$

The meaning of this decomposition becomes evident when we go to Fourier space. First, we define the following convention on Fourier transform, that is, for a function of the comoving coordinates $\mathbf{x}$, $f(\mathbf{x})$, its Fourier transform is defined by [2]

$$f(\mathbf{k}) = \int d^3x f(\mathbf{x}) e^{-i\mathbf{k}\cdot\mathbf{x}} \,, \tag{4.3.6}$$

so

$$f(\mathbf{x}) = \int \frac{d^3k}{(2\pi)^3} f(\mathbf{k}) e^{i\mathbf{k}\cdot\mathbf{x}} \,, \tag{4.3.7}$$

where $\mathbf{k}$ is called the *comoving wavenumber*. Then using this convention, we have the correspondence:

$$\partial_j \leftrightarrow ik_j \,, \tag{4.3.8}$$

thus in Fourier space,

$$h_{0i} \to h_{oi}(\eta, \mathbf{k}) = ik_i B(t, \mathbf{k}) + E_i(\eta, \mathbf{k}) \,, \tag{4.3.9}$$

with $k^i E_i = 0$. It is clear that h_{0i} is decomposed into a longitudinal part with a scalar field B and a transverse part with a vector field E_i.

Next is the space-space component h_{ij}, which is a symmetric 3-tensor with six

[2] Usually, the function $f(\mathbf{k})$ is written as $f(\tilde{\mathbf{k}})$. In this thesis, as long as there is no ambiguity, we omit this notation for the brevity of the formula.

independent components. We decompose it as

$$h_{ij} = -2\delta_{ij}C + \left(\partial_i\partial_j - \frac{1}{3}\delta_{ij}\nabla^2\right) D + \frac{1}{2}\left(\partial_i F_j + \partial_j F_i\right) + h_{ij}^{\rm TT}\,, \tag{4.3.10}$$

where δ_{ij} is the Kronecker delta function and $\nabla^2 = \delta_{ij}\partial^i\partial^j$ is the *flat* space Laplacian, and with the constrains

$$\partial^i F_i = 0\,, \tag{4.3.11}$$

$$\partial^i h_{ij}^{\rm TT} = 0\,, \tag{4.3.12}$$

$$\delta^{ij} h_{ij}^{\rm TT} = 0\,. \tag{4.3.13}$$

In Fourier space, this decomposition becomes

$$h_{ij} = -2\delta_{ij}C - \left(k_i k_j - \frac{1}{3}|\mathbf{k}|^2\delta_{ij}\right) D + \frac{i}{2}(k_i F_j + k_j F_i) + h_{ij}^{\rm TT}\,, \tag{4.3.14}$$

with $k^i F_i = 0$, $k^i h_{ij}^{\rm TT} = 0$, and $\delta^{ij} h_{ij}^{\rm TT} = 0$. That is, we decompose the six independent components of h_{ij} into a "scalar part" by two scalar fields C and D, a "vector part" by a divergence-free vector field F_j, and a "tensor part" by a transverse-traceless tensor field $h_{ij}^{\rm TT}$.

One can prove that there is a one-to-one correspondence between $h_{\mu\nu}$ and the variables $\{A, B, C, D, E_i, F_i, h_{ij}^{\rm TT}\}$ under the boundary conditions that

$$B \to 0\,, \quad D \to 0\,, \quad \nabla^2 D \to 0\,, \quad F_i \to 0\,, \tag{4.3.15}$$

at spatial infinity. Therefore the above scalar-vector-tensor decomposition is an *unique* and *invertible* transformation.

4.3.2 The Dynamical Equation for Tensor Perturbations

In a curved background, the gauge transformation of (4.2.10) will become

$$h_{\mu\nu} \mapsto h'_{\mu\nu} = h_{\mu\nu} - \bar{\nabla}_\mu \xi_\nu - \bar{\nabla}_\nu \xi_\mu\,, \tag{4.3.16}$$

where $\bar{\nabla}_\mu$ is the covariant derivative with respect to the background metric $\bar{g}_{\mu\nu}$, in the current case $\bar{g}_{\mu\nu}$ is the FLRW metric. As mentioned in the last section, the linearized theory is invariant under this gauge transformation. So it is no surprise that not all the variables in the scalar-vector-tensor decomposition have physical degrees of freedom. In fact, it can be shown that the tensor perturbations are *invariant* under the gauge transformation of (4.3.16):

$$h_{ij}^{\mathrm{TT}} = h_{ij}^{\prime\mathrm{TT}} \,. \tag{4.3.17}$$

This means that the two degrees of freedom in tensor perturbations are *physical* degrees of freedom. Furthermore, the *decomposition theorem* states that each type of perturbations (scalar, vector and tensor) evolve independently at *linear* order [29]. Therefore, to determine the evolution of one specific perturbation, we do not need to worry about other types of perturbations, at least in linear order. Let us derive the dynamical equation for tensor perturbations, and we will see that it admits wave-like solutions in a vacuum. These solutions represent cosmological gravitational waves.

The metric which only contains tensor perturbation is

$$ds^2 = -dt^2 + a^2(t)\left(\delta_{ij} + h_{ij}^{\mathrm{TT}}\right) dx^i dx^j \,. \tag{4.3.18}$$

For the convenience of discussion, we also denote the spatial metric as $g_{ij} = a^2(\delta_{ij} + h_{ij}^{\mathrm{TT}})$. What we want is the perturbed Einstein equations:

$$\delta G_\nu^\mu = 8\pi G\, \delta T_\nu^\mu \,, \tag{4.3.19}$$

where $\delta G_\nu^\mu = \delta R_\nu^\mu + \bar{g}_{\mu\nu}\delta R$. First, we need to compute the Christoffel symbol $\Gamma_{\mu\nu}^\lambda$ in

linear order of $h_{\mu\nu}$, the result is

$$\Gamma^0_{00} = 0 = \Gamma^0_{i0} = \Gamma^i_{00}\,; \tag{4.3.20}$$

$$\Gamma^0_{ij} = H g_{ij} + \frac{a^2}{2}\partial_0 h^{\rm TT}_{ij}\,; \tag{4.3.21}$$

$$\Gamma^i_{0j} = H\delta_{ij} + \frac{1}{2}\partial_0 h^{\rm TT}_{ij}\,; \tag{4.3.22}$$

$$\Gamma^i_{jk} = \frac{1}{2}\left(\partial_j h^{\rm TT}_{ik} + \partial_k h^{\rm TT}_{ij} - \partial_i h^{\rm TT}_{jk}\right)\,. \tag{4.3.23}$$

Note that the index of $h^{\rm TT}_{ij}$ and its derivatives $\partial_k h^{\rm TT}_{ij}$ are raised and lowered by δ^{ij} and δ_{ij}, so there is no difference between the up and down index in them.

Then from the Christoffel symbol, we can compute the Ricci tensor $R_{\mu\nu}$, but what we need is only the spatial-spatial components R_{ij} that contain the tensor perturbation. From its definition

$$\begin{aligned} R_{ij} &\equiv R^{\alpha}{}_{i\alpha j} \\ &= \partial_\alpha \Gamma^\alpha_{ij} - \partial_j \Gamma^\alpha_{i\alpha} + \Gamma^\alpha_{\alpha\beta}\Gamma^\beta_{ij} - \Gamma^\alpha_{j\beta}\Gamma^\beta_{\alpha i}\,, \end{aligned} \tag{4.3.24}$$

one obtains

$$R_{ij} = \left(2H^2 + \frac{\ddot{a}}{a}\right) g_{ij} + \frac{3}{2}a^2 H\,\partial_0 h^{\rm TT}_{ij} + \frac{a^2}{2}\,\partial_0\partial_0 h^{\rm TT}_{ij} - \frac{1}{2}\,\nabla^2 h^{\rm TT}_{ij}\,. \tag{4.3.25}$$

The curvature scalar R is

$$R \equiv g^{\mu\nu}R_{\mu\nu} = g^{ij}R_{ij} = \frac{3}{a^2}\left(2H^2 + \frac{\ddot{a}}{a}\right)\,, \tag{4.3.26}$$

and it does not contain any linear tensor perturbations. Therefore the left-hand side of the perturbed Einstein equation (4.3.19) becomes $\delta R^i{}_j$. From equation (4.3.25) and relation $R^i{}_j = g^{ik}R_{kj}$, one obtain

$$\delta G^i{}_j = \frac{1}{2}\delta^{ik}\left(3H\,\partial_0 h^{\rm TT}_{kj} + \partial_0\partial_0 h^{\rm TT}_{kj} - \frac{1}{a^2}\nabla^2 h^{\rm TT}_{kj}\right)\,. \tag{4.3.27}$$

We can do a similar decomposition in the energy-momentum tensor $T_{\mu\nu}$. The

tensor part in the decomposition corresponds to the anisotropic stress of cosmological constitutes. The most significant contribution to this term is the anisotropic neutrino stress. In this thesis, we will neglect it and set the right-hand side of equation (4.3.19) to zero for the tensor perturbations.

According to the constrains (4.3.12) and (4.3.13), the two independent components in tensor perturbation are traceless and transverse to the wave vector $\hat{\mathbf{k}}$. Specialize to the case $\hat{\mathbf{k}} = \hat{\mathbf{e}}_z$, and write h_{ij}^{TT} as

$$h_{ij}^{\mathrm{TT}} = \begin{pmatrix} h_+ & h_\times & 0 \\ h_\times & -h_+ & 0 \\ 0 & 0 & 0 \end{pmatrix}, \tag{4.3.28}$$

then from $\delta G^1{}_1 - \delta G^2{}_2 = 0$ one obtain

$$3H\partial_0 h_+ + \partial_0\partial_0 h_+ - \frac{1}{a^2}\nabla^2 h_+ = 0\,, \tag{4.3.29}$$

and $h_\times$ obey the same equation. Change to the conformal time η so that $\partial_0 = a^{-1}d/(d\eta)$, then equation (4.3.29) become

$$h_P^{''} + 2\frac{a^{'}}{a}h_P^{'} - \nabla^2 h_P = 0\,, \tag{4.3.30}$$

where $P = +, \times$. These are the evolution equation for the tensor perturbations in the FRLW spacetime.

4.4 The Generation of Primordial GWs During Inflation

The standard inflation scenario supposes that the universe consists of a uniform and yet unknown (but could be the scalar field we introduced in Section 3.3) inflation

field and a uniform spacetime field described by the FLRW metric during the inflation period. Upon these uniform backgrounds, there are perturbations, i.e., quantum fluctuations in these fields. In particular, the quantum fluctuations of tensor perturbation seed the inflationary primordial GWs that we are interested in this thesis. In this section, we quantify the quantum fluctuations of tensor perturbation.

One crucial point about the initial quantum fluctuations is that they are *stochastic* variables. This is because no known theory can predict for instance the initial value of the tensor perturbation $h_{ij}(\eta_{\rm in}, \mathbf{x})$ at a specific point $\mathbf{x}$ in space. We can only predict and measure the statistical properties of these stochastic variables, for example, their mean values and correlators. While the mean value of the perturbation, $\langle h_{ij}(\eta_{\rm in}, \mathbf{x})\rangle$ [3], can be set to zero, the variance, i.e. the average of the square of the perturbation, can not be set to zero. Therefore, the variance of the perturbations is observable.

It is not unreasonable to assume that the generation of the perturbation is a Gaussian random process according to the *central limit theorem*, which asserts that the sum of a large number of independent random processes will result in a Gaussian random process. Under the assumption of Gaussian perturbation, all the non-trivial information about the initial tensor perturbation is contained in the two-point correlator $\langle h_{\rm P}(\eta_{\rm in}, \mathbf{x})\, h_{\rm P'}(\eta_{\rm in}, \mathbf{x}')\rangle$ because any higher-order correlator can be reduced to the sum of the two-point correlator (see, for example, Section 3.3.4 in [19] for a proof). Any sign of non-Gaussianity is undoubtedly valuable because it could contain information about the specific mechanism for generating primordial perturbations. However, since present cosmological observations are consistent with the Gaussian initial fluctuations, we will assume a Gaussian initial condition in this section.

In this section, we also assume that the background spacetime is homogeneous and isotropic, i.e. the FLRW spacetime. It does not have to be so because there are inflation models that would break this assumption, but for the present discussion, we would like to maintain this standard assumption. Homogeneous and isotropy means that the background is invariant under spatial translations and rotations, which im-

[3] The symbol $\langle ... \rangle$ represents the ensemble average; see Section 5.4.2 for its meaning in cosmology.

plies that the two-point correlator of perturbation $\langle h(\eta_{\rm in}, \mathbf{x})\, h(\eta_{\rm in}, \mathbf{x}')\rangle$ [4] only depends on a function of $|\mathbf{x}-\mathbf{x}'|$, i.e.,

$$\langle h(\eta_{\rm in}, \mathbf{x})\, h(\eta_{\rm in}, \mathbf{x}')\rangle = f(|\mathbf{x}-\mathbf{x}'|)\,. \tag{4.4.1}$$

It is usually more convenient to work with the Fourier modes because, according to relation (4.3.8), the derivative operation can be simply replaced by the multiplication of a factor. Therefore, under the convention of (4.3.6) and (4.3.7), the two-point correlator of equation (4.4.1) becomes to

$$\langle h_{\rm P}(\eta_{\rm in}, \mathbf{k})\, h^*_{\rm P'}(\eta_{\rm in}, \mathbf{k}')\rangle = (2\pi)^3\, \delta^{(3)}(\mathbf{k}-\mathbf{k}')\, \delta_{\rm PP'}\, P_{h,{\rm in}}(k)\,. \tag{4.4.2}$$

All non-trivial information about the initial tensor perturbations now is contained in the function $P_{h,{\rm in}}(k)$, which is called the *power spectrum* of the primordial tensor perturbations. Now let us compute this function.

First we write the equation (4.3.30) in Fourier space, then it becomes

$$h''(\eta, \mathbf{k}) + 2\frac{a'}{a}h'(\eta, \mathbf{k}) + k^2 h(\eta, \mathbf{k}) = 0\,. \tag{4.4.3}$$

We have dropped the polarisations' subscript P for clarity. Then define a new variable $\mathsf{h}(\eta, \mathbf{k})$ as

$$\mathsf{h} \equiv \frac{ah}{\sqrt{16\pi G}}\,. \tag{4.4.4}$$

Under the above definition, equation (4.4.3) is simplified as

$$\frac{1}{a}\left[\mathsf{h}'' + \left(k^2 - \frac{a''}{a}\right)\mathsf{h}\right] = 0\ , \tag{4.4.5}$$

and the equation in the bracket has the same form as the equation governing the motion of a harmonic oscillator with frequency ω: $\ddot{x}+\omega^2 x = 0$. Therefore, in analogy to the procedure of quantizing the harmonic oscillator, we could write down the

[4] For convenience, we have omit the index of polarization.

quantum operator for $\mathsf{h}(\eta, \mathbf{k})$ as follows:

$$\hat{\mathsf{h}}(\eta, \mathbf{k}) = \chi(\eta, k)\, \hat{a}_{\mathbf{k}} + \chi^{*}(\eta, k)\, \hat{a}^{\dagger}_{\mathbf{k}}\,, \tag{4.4.6}$$

where $\hat{a}_{\mathbf{k}}$ and $\hat{a}^{\dagger}_{\mathbf{k}}$ are the *annihilation* and the *creation* operator correspondingly. The annihilation operator annihilates the *vacuum* state $|0\rangle$ (or no-particle state) in a sence that is: $\hat{a}_{\mathbf{k}}\,|0\rangle = 0$ for any mode $\mathbf{k}$. On the other hand, the creation operator acting on the vacuum state leads to a one-particle state, that is, $\hat{a}^{\dagger}_{\mathbf{k}}\,|0\rangle = |1_{\mathbf{k}}\rangle$. As a requirement of the canonical quantization procedure, the annihilation and creation operators also should satisfy the following commutation relations:

$$[\hat{a}_{\mathbf{k}}, \hat{a}^{\dagger}_{\mathbf{k}'}] \equiv \hat{a}_{\mathbf{k}}\hat{a}^{\dagger}_{\mathbf{k}'} - \hat{a}^{\dagger}_{\mathbf{k}'}\hat{a}_{\mathbf{k}} = \delta_{\mathbf{k}\mathbf{k}'}\,; \tag{4.4.7}$$

$$[\hat{a}_{\mathbf{k}}, \hat{a}_{\mathbf{k}'}] = 0\,; \tag{4.4.8}$$

$$[\hat{a}^{\dagger}_{\mathbf{k}}, \hat{a}^{\dagger}_{\mathbf{k}'}] = 0\,. \tag{4.4.9}$$

The coefficients of the annihilation and creation operators satisfy

$$\chi^{''}(\eta, k) + \left(k^2 - \frac{a^{''}}{a}\right)\chi(\eta, k) = 0\,. \tag{4.4.10}$$

Now we can compute the quantum fluctuations of the operator $\hat{\mathsf{h}}$ in the ground state $|0\rangle$ (i.e., the vacuum expectation value of $\hat{\mathsf{h}}$):

$$\begin{aligned} \langle|\hat{\mathsf{h}}|^2\rangle &= \langle 0|\hat{h}^{\dagger}\hat{h}|0\rangle \\ &= \langle 0|\,(\chi^{*}\hat{a}^{\dagger}_{\mathbf{k}} + \chi\hat{a}_{\mathbf{k}})\,(\chi\hat{a}_{\mathbf{k}} + \chi^{*}\hat{a}^{\dagger}_{\mathbf{k}})\,|0\rangle\,. \end{aligned} \tag{4.4.11}$$

According to the communication relation (4.4.7) and the definition of annihilation operator, the above equation reduces to

$$\langle|\hat{\mathsf{h}}|^2\rangle = |\chi(\eta, k)|^2\,; \tag{4.4.12}$$

Changing the variable back to h, we then find that

$$\langle \hat{h}^{\dagger}(\eta, \mathbf{k})\, \hat{h}(\eta, \mathbf{k}) \rangle = \frac{16\pi G}{a^2(\eta)} \left| \chi(\eta, k) \right|^2 . \tag{4.4.13}$$

When the (conformal) time is taken to be in the inflation, this is just the primordial power spectrum of the tensor perturbations defined in (4.4.2).

To obtain the solution of $\chi(\eta, k)$ in equation (4.4.10), we need to determine the scale factor and its derivative during inflation. Before doing that, let us redefine the conformal time variable η by setting its origin, $\eta = 0$, at the end of inflation. That is,

$$\eta = \int_{t_{\rm end}}^{t} \frac{dt'}{a(t')} , \tag{4.4.14}$$

where $t_{\rm end}$ represents the cosmic time at the end of inflation. Under this convention, $t > t_{\rm end}$ (or $\eta > 0$) accounts for the period after inflation, while $t < t_{\rm end}$ (or $\eta < 0$) represent the period of inflation. The reason we do this is that during inflation, the conformal time becomes very large and then changes relatively little in the following radiation- and matter-dominated eras; if we take the lower integral limit in (4.4.14) to be $t = 0$, the conformal time would not be an effective time parameter to describe the period after inflation. Under this convention, the conformal time during inflation can be calculated as

$$\eta = \int_{t_{\rm end}}^{t_{\rm in}} \frac{dt'}{a(t')} = \int_{a_{\rm end}}^{a_{\rm in}} \frac{1}{Ha^2} da \cong -\frac{1}{a_{\rm in} H} , \tag{4.4.15}$$

where we have used the fact that H is nearly constant during inflation; $a_{\rm in}$ represents the scale factor at some moment in inflation. Form equation (4.4.15), we obtain $a^{'} \equiv da/(d\eta) \cong -a/\eta$ and $a^{''} \cong 2a/\eta^2$, therefore $a^{''}/a \cong 2/\eta^2$. Thus the equation for $\chi(\eta, k)$ becomes

$$\chi^{''}(\eta, k) + \left(k^2 - \frac{2}{\eta^2} \right) \chi(\eta, k) = 0 . \tag{4.4.16}$$

The initial conditions for the above equation are obtained by considering the situation at very early times, and the mode is far inside the horizon, i.e., $1/k \ll$

$|1/(aH)|$. Using relation (4.4.15), this is equal to

$$k \gg \frac{1}{|\eta|} \quad \text{(sub-horizon condition)}\,. \tag{4.4.17}$$

Then the k^2 term dominates, and the equation (4.4.16) reduces to the equation of the simple harmonic oscillator which possess a normalized solution $e^{-ik\eta}/\sqrt{2k}$. This initial condition enables us to determine the appropriate solution to equation (4.4.16); the solution is

$$\chi(\eta, k) = \frac{e^{-ik\eta}}{\sqrt{2k}} \left(1 - \frac{i}{k\eta}\right)\,. \tag{4.4.18}$$

However, the perturbation is not always inside the horizon. In comoving coordinates, the wavelength of perturbation is constant while the Hubble radius decrease during inflation. Therefore, all the initial perturbations would become super-horizon modes at the end of inflation, i.e., $1/k \gg |1/(aH)|$, that is

$$k|\eta| \ll 1 \quad \text{(super-horizon condition)}\,; \tag{4.4.19}$$

take this limit of equation (4.4.18), we obtain

$$\lim_{k|\eta|\ll 1} \chi(\eta, k) = \frac{e^{-ik\eta}}{\sqrt{2k}} \left(-\frac{i}{k\eta}\right)\,. \tag{4.4.20}$$

Finally, the primordial power spectrum of GWs can be calculated from (4.4.13), which results in

$$P_h(\eta_{\rm in}, k) \equiv \langle \hat{h}^\dagger(\eta_{\rm in}, \mathbf{k})\, \hat{h}(\eta_{\rm in}, \mathbf{k}) \rangle = \frac{1}{a^2} \frac{8\pi G}{k^3 \eta_{\rm in}^2} = \frac{8\pi G H^2}{k^3}\,. \tag{4.4.21}$$

CHAPTER 5

Antipodal Angular Correlations (AAC) of the Inflationary SGWB

From this chapter, we begin to study a unique and universal property of the inflationary SGWB: the antipodal angular correlations (AAC). Since primordial GWs are expected to be observed as one kind of stochastic background, in Section 5.1, we briefly review how to characterize an SGWB in general. In Section 5.2, we examine the evolution of primordial GWs by comparing their wavelength with the scale of the universe. In Section 5.3, we derive the AAC of inflationary SGWB as a natural result when the super-horizon mode re-enters the horizon. In Section 5.4, we discuss the detectability of the AAC property, both in frequency and time domain analysis.

5.1 Stochastic Gravitational-wave Background

The discovery of CMB is one of the most significant in the history of cosmology. Just like electromagnetic waves, it is not unreasonable to expect that a stochastic background of GWs also permeates the universe. Such a SGWB might emerge from the processes that took place in the early universe, such as the inflation models [12, 80, 16], cosmic strings [43, 27, 77, 73], pre-Big-Bang models [50, 22, 21] and many others [13]; we shall call such a gravitational wave background the *cosmological SGWB*. An SGWB might also emerge from an incoherence superposition of unresolved GWs that was generated by a large number of compact objects such as black-hole or neutron star binaries [69, 30], supernovae [23], and magnetars [24]; we shall call it the

astrophysical SGWB. In preparation for studying the inflationary SGWB later, in this section, we introduce how to characterize an SGWB generally. Two main references of this section are [15] and [47].

We say the gravitational waves are stochastic in the sense that their properties can be characterized only *statistically*. The starting point to quantify this type of GWs is a plane wave expansion for the tensor perturbations in a TT gauge:

$$h_{ij}^{\mathrm{TT}}(t,\mathbf{x}) = \sum_{P=+,\times} \int_{-\infty}^{\infty} df \int_{S^2} d^2\hat{\mathbf{n}}\, h_P(f,\hat{\mathbf{n}})\, e_{ij}^P(\hat{\mathbf{n}})\, e^{-i2\pi f(t-\hat{\mathbf{n}}\cdot\mathbf{x})}\,. \tag{5.1.1}$$

Here $\hat{\mathbf{n}}$ is a unit vector specifying the propagation direction of a wave. The frequency f is defined by the wave vector $\mathbf{k}$ through $\mathbf{k} \equiv 2\pi f\hat{\mathbf{n}}$. Of course, a physical frequency of a wave is non-negative; here, the negative value of f does not mean negative energy but represents the wave propagating in the opposite direction of $\hat{\mathbf{n}}$. The *polarization tensors* $e_{ij}^P(\hat{\mathbf{n}})$ (with $P = +, \times$ representing the polarizations) are defined as

$$e_{ij}^+(\hat{\mathbf{n}}) = \hat{\mathbf{u}}_i\hat{\mathbf{u}}_j - \hat{\mathbf{v}}_i\hat{\mathbf{v}}_j\,, \tag{5.1.2}$$

$$e_{ij}^\times(\hat{\mathbf{n}}) = \hat{\mathbf{u}}_i\hat{\mathbf{v}}_j + \hat{\mathbf{v}}_i\hat{\mathbf{u}}_j\,, \tag{5.1.3}$$

where $\hat{\mathbf{u}}$ and $\hat{\mathbf{v}}$ are two unit vectors orthogonal to the propagation direction $\hat{\mathbf{n}}$ and to each other. The reality of $h_{ij}(t,\mathbf{x})$ implies that the Fourier amplitudes $h_P(f,\hat{\mathbf{n}})$ satisfy

$$h_P(f,\hat{\mathbf{n}}) = h_P^*(-f,\hat{\mathbf{n}})\,, \tag{5.1.4}$$

where $*$ denotes the complex conjugation.

Then a stochastic gravitational wave is *defined* by the situation that the amplitudes $h_A(f,\hat{\mathbf{n}})$ (and therefore $h_{ij}(t,\mathbf{x})$) are *random variables*. The properties of stochastic gravitational waves are characterized by the mean value $\langle h_P(f,\hat{\mathbf{n}})\rangle$, the two-point correlator $\langle h_P^*(f_1,\hat{\mathbf{n}}_1)\, h_{P'}(f_2,\hat{\mathbf{n}}_2)\rangle$, and so on.

We can make some additional statistic assumptions on the SGWB as well. For example:

- The background is stationary. This means that all statistical quantities do

not depend on the choice of time origin but only on the time differences. For instance, a two-point correlator $\langle h(t_1, \mathbf{x}_1)\, h(t_2, \mathbf{x}_2)\rangle$ [1] can only depend on $t_1 - t_2$. In Fourier space, this means that $\langle h_P^*(f_1, \hat{\mathbf{n}}_1)\, h_{P'}(f_2, \hat{\mathbf{n}}_2)\rangle$ is proportional to $\delta(f_1 - f_2)$.

- The background is a Gaussian random process. This means that the mean value $\langle h_P(f, \hat{\mathbf{n}})\rangle$ and the two-point correlator $\langle h_P^*(f_1, \hat{\mathbf{n}}_1)\, h_{P'}(f_2, \hat{\mathbf{n}}_2)\rangle$ completely specify the statistical properties of the background.

- The background is unpolarized. This means that statistically speaking, the background contains equivalent + and × polarization components. In this case, the two-point correlator $\langle h_P^*(f_1, \hat{\mathbf{n}}_1)\, h_{P'}(f_2, \hat{\mathbf{n}}_2)\rangle$ is proportional to $\delta_{PP'}$ and the proportionality coefficient must be independent of the polarization index P.

- The background has no angular correlations. In this case, for instance, the two-point correlator $\langle h_P^*(f_1, \hat{\mathbf{n}}_1)\, h_{P'}(f_2, \hat{\mathbf{n}}_2)\rangle$ is proportional to a Dirac delta function $\delta^2(\hat{\mathbf{n}}_1, \hat{\mathbf{n}}_2)$ which is defined as

$$\delta^2(\hat{\mathbf{n}}_1, \hat{\mathbf{n}}_2) = \delta(\phi_1 - \phi_2)\, \delta(\cos\theta_1 - \cos\theta_2)\,, \tag{5.1.5}$$

  where (θ, ϕ) are the polar angles of $\hat{\mathbf{n}}$.

- The background is (statistical) isotropic [2]. This condition means that all correlation functions have no angular dependence. For instance, the two-point correlator $\langle h_P^*(f_1, \hat{\mathbf{n}}_1)\, h_{P'}(f_2, \hat{\mathbf{n}}_2)\rangle$ depends on $\hat{\mathbf{n}}_1$ and $\hat{\mathbf{n}}_2$ only through $\hat{\mathbf{n}}_1 \cdot \hat{\mathbf{n}}_2$.

To a first approximation, we may assume that a cosmological SGWB is an *unpolarized, stationary Gaussian random process* and *does not possess any angular correlation*. These assumptions can be justified as follows.

The central limit theorem states that the sum of a large number of statistically independent events produce a Gaussian random process, independent of the prob-

[1] For the sake of brevity, we omit the index.

[2] Note that statistical isotropy does not forbid angular correlations. For example, the map of CMB temperature is isotropic but also has angular correlations.

ability distributions of individual events. For many early universe processes which happened randomly on each spacetime point, the produced SGWB should be Gaussian. However, for an astrophysical background that is the sum of a few GW events' signals, the assumption of Gaussian will not be true.

To a first approximation, the CMB does not possess any angular correlations; therefore, it is reasonable to assume that a gravitational wave background produced in the early universe would also be like this.

The typical time scale in which a cosmological SGWB would change is the order of the age of the universe, and it is much longer than the real observation times. It is unlikely that the cosmological SGWB would change dramatically during an observational time. Thus the assumption of stationary is reasonable.

Also, there is no solid theoretical reason why a stochastic background should be polarized.

However, a cosmological SGWB could be anisotropic, either because it has an intrinsic anisotropy, like the inflationary SGWB we will discuss later, or because of its propagation in the inhomogeneous universe.

Under the above assumptions, the statistical properties of an SGWB is *completely* determined by two quantities: the expectation value $\langle h_P(f,\hat{\mathbf{n}})\rangle$ and the two-point correlator $\langle h_P^*(f,\hat{\mathbf{n}}_1)\, h_{P'}(f',\hat{\mathbf{n}}_2)\rangle$. Furthermore, the two-point correlation function satisfies

$$\langle h_P^*(f,\hat{\mathbf{n}}_1)\, h_{P'}(f',\hat{\mathbf{n}}_2)\rangle = \delta(f-f')\,\delta_{PP'}\,\delta^2(\hat{\mathbf{n}}_1,\hat{\mathbf{n}}_2)\,\frac{1}{2}S_h(f)\,, \tag{5.1.6}$$

where the function $S_h(f)$ is called the (single-sided) *spectral density* of the stochastic background.

It is convenient to characterize an SGWB by a dimensionless quantity $\Omega_{\rm gw}$ which describes the ratio of the SGWB's energy density to the total energy density of the universe:

$$\Omega_{\rm gw} \equiv \frac{\rho_{\rm gw}}{\rho_{\rm cr}}\,. \tag{5.1.7}$$

Here, $\rho_{\rm cr}$ is called the *critical density* of the universe, and it is defined by the current

Hubble constant H_0 :

$$\rho_{\rm cr} = \frac{3H_0^2}{8\pi G}\,. \tag{5.1.8}$$

Because the universe is observed to be spatially flat with good accuracy [10], the critical density can be taken as the present energy density. Also, $\rho_{\rm gw}$ represents the energy density of gravitational wave; it is related to $h_{ij}(t,\mathbf{x})$ by (see, e.g., Section 35.7 of Ref. [56])

$$\rho_{\rm gw} = \frac{1}{32\pi G}\langle \dot{h}_{ij}\dot{h}^{ij}\rangle\,. \tag{5.1.9}$$

In the literature, one often *defines* the background energy density as a function of frequency $\Omega_{\rm gw} = \Omega_{\rm gw}(f)$ by

$$\Omega_{\rm gw}(f) \equiv \frac{f}{\rho_{\rm cr}}\frac{d\rho_{\rm gw}}{df}\,, \tag{5.1.10}$$

where $d\rho_{\rm gw}$ represent the energy density of gravitational wave contained in the frequency range f to $f+df$. Such a definition is convenient in an observational search for the SGWB. Still, we should remember that generally, the energy density defined in equation (5.1.7) may also depend on directions.

Current observational constraints on the isotropic SGWB came from the first observing run on the Advanced Laser Interferometer Gravitational Wave Observatory (aLIGO) [4]. The result shows that the energy density of the stochastic background is constrained to be $\Omega_0 < 1.7\times 10^{-7}$ in the frequency band $20-86\,\mathrm{Hz}$, assuming a flat energy density spectrum. Here, Ω_α (where α is a real number) is defined by

$$\Omega_{\rm gw} = \Omega_\alpha\left(\frac{f}{f_{\rm ref}}\right)^\alpha\,, \tag{5.1.11}$$

and $f_{\rm ref}$ is the reference frequency.

5.2 Evolution of the Primordial GWs

5.2.1 Evolution of the Scale of the Universe

To examine the evolution of the primordial GWs, the relation between the tensor perturbation's size and the universe's local scale is essential. In this subsection, we examine the evolution of the scale of the universe.

The local scale of the universe is described by the (comoving) Hubble radius [3] $\mathcal{H}^{-1}$ which we defined in equation (2.2.5), and it is determined by the Friedmann equation written in the comoving coordinates

$$\mathcal{H}^2(\eta) = \frac{8\pi G}{3} a^2 \rho_{\rm tot}(\eta)\,, \tag{5.2.1}$$

where $\rho_{\rm tot}$ represents the total energy density of all components in the universe, and it is given by

$$\rho_{\rm tot}(\eta) = \sum_{\lambda} \rho_{\lambda}(\eta)\,. \tag{5.2.2}$$

Here λ represents each specie of the component. The conservation of the total energy-momentum tensor gives a relation between the total energy density and the total pressure $p_{\rm tot}$:

$$\rho'_{\rm tot} + 3\mathcal{H}(\rho_{\rm tot} + p_{\rm tot}) = 0\,, \tag{5.2.3}$$

where $p_{\rm tot}$ is equal to

$$p_{\rm tot}(\eta) = \sum_{\lambda} w_{\lambda}(\eta)\, \rho_{\lambda}(\eta)\,. \tag{5.2.4}$$

The minimal components of the universe are known to be photons, neutrinos, baryons, cold dark matter, and a cosmological constant. We describe these components simply as radiation, matter, and a cosmological constant; therefore

$$\rho_{\rm tot} = \rho_{\rm R} + \rho_{\rm M} + \rho_{\Lambda}\,. \tag{5.2.5}$$

Furthermore, we assume that the interaction rates in the processes that exchange

[3] To examine the evolution of the universe, it is often convenient to work in the comoving frame.

the energy between different components are much smaller than the Hubble rate $\mathcal{H}$. Under this assumption, the conservation equation for the total energy-momentum tensor (5.2.3) can be separated into the conservation equations for each component:

$$\rho_\lambda' + 3\mathcal{H}(1+w_\lambda)\rho_\lambda = 0\,. \tag{5.2.6}$$

In terms of the scale factor, the solution of the above equation is

$$\rho_\lambda(a) = \rho_{\lambda,0}\, a^{-3(1+w_\lambda)}\,, \tag{5.2.7}$$

where the integral constant $\rho_{\lambda,0}$ represents the energy density of the component λ in the present time. In cosmology, $\rho_{\lambda,0}$ is often compared with the critical density today $\rho_0 = 3H_0^2/(8\pi G)$ and written as the energy fractions Ω_λ, that is

$$\Omega_\lambda \equiv \frac{\rho_{\lambda,0}}{\rho_0}\,. \tag{5.2.8}$$

Then the energy density for each component are

$$\rho_{\rm R} = \rho_0\,\Omega_{\rm R}\,a^{-4}\,;\quad \rho_{\rm M} = \rho_0\,\Omega_{\rm M}\,a^{-3}\,;\quad \rho_\Lambda = \rho_0\,\Omega_\Lambda\,. \tag{5.2.9}$$

Substituting (5.2.9) into (5.2.1), one obtain

$$\mathcal{H} = H_0 a\left[\Omega_{\rm R}a^{-4} + \Omega_{\rm M}a^{-3} + \Omega_\Lambda\right]^{\frac{1}{2}}\,. \tag{5.2.10}$$

From the current observations, we could determine the energy fraction for each component Ω_λ; then equation (5.2.10) tells us the evolution of the scale of the universe.

As we go to the past, the first two terms in the bracket of equation (5.2.10) dominate, and we may neglect the cosmological constant term when estimating the scale of the universe in the past. Also, an important moment in the history of the universe is the transition between radiation dominance and matter dominance. This moment, called the *RD-MD equilibrium*, is given by the condition $\rho_{\rm R} = \rho_{\rm M}$; from

(5.2.9) this implies $a_{\rm eq} = \Omega_{\rm R}/\Omega_{\rm M}$. Then using $\mathcal{H} = a'/a$, equation (5.2.10) becomes

$$\frac{da}{d\eta} \simeq H_0 \Omega_{\rm R}^{\frac{1}{2}} \left(1 + \frac{a}{a_{\rm eq}}\right)^{\frac{1}{2}} . \tag{5.2.11}$$

Treating $a/a_{\rm eq}$ as a new variable, one obtains the solution of the above equation:

$$\left(\frac{a}{a_{\rm eq}} + 1\right)^{\frac{1}{2}} = \frac{\eta}{\eta_*} + \left(\frac{a_{\rm end}}{a_{\rm eq}} + 1\right)^{\frac{1}{2}} , \tag{5.2.12}$$

where $\eta_* \equiv \frac{2\Omega_{\rm R}^{1/2}}{H_0 \Omega_{\rm M}}$, and $a_{\rm end}$ represents the scale factor at the end of inflation. Since it is much smaller than the scale factor at RD-MD equilibrium, we can also neglect the $a_{\rm end}/a_{\rm eq}$ term in (5.2.12) ; thus $a(\eta)$ can be approximated as

$$a(\eta) \simeq \left[\frac{2\eta}{\eta_*} + \left(\frac{\eta}{\eta_*}\right)^2\right] a_{\rm eq} . \tag{5.2.13}$$

Finally, we obtain an approximate formula of the Hubble radius $\mathcal{H}^{-1}$ in the past universe:

$$\mathcal{H}^{-1} = \frac{\eta(\eta + 2\eta_*)}{2(\eta + \eta_*)} . \tag{5.2.14}$$

Letting $a(\eta) = a_{\rm eq}$ in equation (5.2.13), we obtain the conformal time at the RD-MD equilibrium

$$\eta_{\rm eq} = \left(\sqrt{2} - 1\right) \eta_* . \tag{5.2.15}$$

Deep in the radiation dominant, $\eta \ll \eta_*$, equation (5.2.14) gives $\mathcal{H}^{-1} \simeq \eta$, while deep in the matter dominant, $\eta \gg \eta_*$, equation (5.2.14) then gives $\mathcal{H}^{-1} \simeq \eta/2$. On the other hand, from (4.4.15), we get the comoving Hubble radius during inflation, $\mathcal{H}^{-1} = -\eta$. In summary, in comoving coordinates, the scale of the universe evolves as

$$\mathcal{H}^{-1} \propto \begin{cases} -\eta & \text{inflation} ; \\ \eta & \text{deep in RD} ; \\ \frac{1}{2}\eta & \text{deep in MD} . \end{cases} \tag{5.2.16}$$

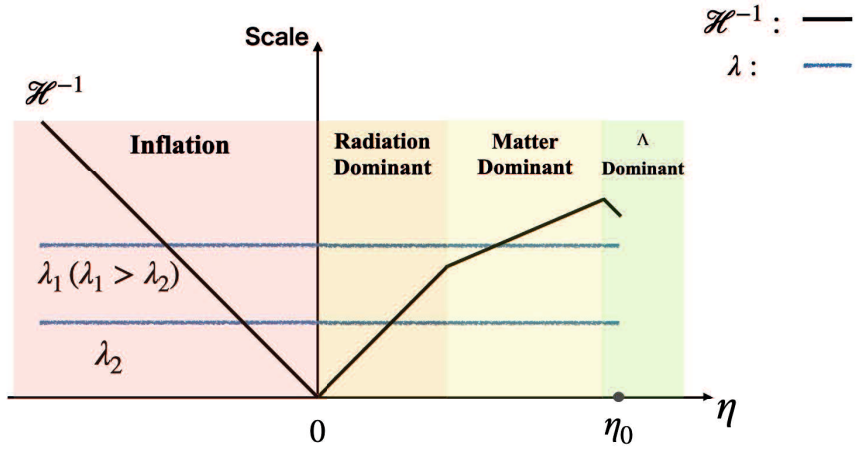

Fig. 5.2.1: Comparing the tensor perturbations' scales and the universe's size in comoving coordinates.

5.2.2 Evolution of Primordial GWs in the Homogeneous Universe

Knowing how the universe's scale changes, let us compare this scale with the size of the tensor perturbations. In the comoving frame, the comoving wavelength of the perturbation, $\lambda = 2\pi/k$ (where $k = |\mathbf{k}|$), is invariant. We then sketch these two scales in Figure 5.2.1.

We see that in Figure 5.2.1 there are regions in which the perturbation size is much smaller than the local scale of the universe: the beginning of inflation and some areas in RD and MD. In these regions, we say that the perturbation is in the *sub-horizon regime* and the mode of perturbation is a *sub-horizon mode*. This situation is equivalent to the condition:

$$k \gg \mathcal{H}(\eta)\,, \tag{5.2.17}$$

or in terms of the physical wavelength $\lambda_{\rm ph} = a(t)\lambda$,

$$\frac{\lambda_{\rm ph}}{2\pi} \ll H^{-1}(t)\,. \tag{5.2.18}$$

On the other hand, there are regions in which the perturbation size could be much larger than the local scale of the universe. We call these regimes the *super-horizon regime* and the perturbation in such regime the *super-horizon mode*. The condition for the super-horizon mode can be written as

$$k \ll \mathcal{H}(\eta)\,. \tag{5.2.19}$$

We see that in the inflation scenario, the initial perturbations can be generated in the sub-horizon regime to explain the causal relation of the late-time structure of the universe. The statistical property of the initial tensor perturbations is given by the primordial power spectrum (4.4.21) that we introduced in the last chapter. Then the Hubble radius shrinks as inflation continues; the perturbation size is comparable to the universe's local dimension and eventually becomes larger. The primordial sub-horizon tensor perturbations thus become super-horizon modes. At this time, these modes lose their quantum nature and become classical. After the inflation has ended, the (comoving) Hubble radius begins to expand. When the Hubble radius is comparable and again becomes larger than the perturbation size, the modes in the super-horizon region cross the horizon and become sub-horizon modes once again. The moment at which super-horizon modes become sub-horizon modes is called the *horizon re-entry*. After re-entering the horizon, the primordial tensor perturbations propagate to us as gravitational waves.

Now let us consider a classicalized super-horizon mode deep in the RD to set up the initial conditions for the late-time sub-horizon mode. We make the following assumptions about the super-horizon mode $h_{ij}(\eta, \mathbf{x})$. We assume that it can be expanded as [85, 71]

$$h_{ij}(\eta, \mathbf{x}) \equiv \int \frac{d^3k}{(2\pi)^3}\, \mathtt{h}_P^{\rm pri}(\mathbf{k})\, h(\eta, k)\, e_{ij}^P(\hat{\mathbf{n}})\, e^{i\mathbf{k}\cdot\mathbf{x}}\,, \tag{5.2.20}$$

where $\mathtt{h}_P^{\rm pri}(\mathbf{k}) \equiv h_P(\eta_{\rm in}, \mathbf{k})$ represents the primordial stochastic tensor perturbations and its property is determined by the primordial power spectrum of (4.4.2). The

evolution of the super-horizon mode is described by the *transfer function* $h(\eta, k)$. The equation of motion for the transfer function is the dynamical equation of tensor perturbation (4.4.3) that we derived in Chapter 4; we rewrite it here for convenience in our later discussion:

$$h^{''}(\eta, k) + 2\frac{a^{'}}{a}h^{'}(\eta, k) + k^2 h(\eta, k) = 0\,. \tag{5.2.21}$$

In comoving coordinates, the scale factor in RD evolves as $a(\eta) \propto \eta$; the factor $2a^{'}/a$ in (5.2.21) then becomes $2/\eta$. Also, in the super-horizon regime, $k \ll \mathcal{H}$, we can neglect the third term in equation (5.2.21), and the equation becomes

$$h''(\eta, k) + \frac{2}{\eta}h'(\eta, k) \simeq 0\,. \tag{5.2.22}$$

This equation has two independent solutions: a constant mode solution and a decaying mode solution $h(\eta, k) \propto 1/\eta$. We only focus on the constant mode because it is the mode that would propagate to us. The initial conditions for the later evolution of the sub-horizon modes, therefore, can be set as

$$h(\eta_{\rm sup}, k) = h_{\rm sup}(k)\,; \tag{5.2.23}$$

$$h'(\eta_{\rm sup}, k) = 0\,. \tag{5.2.24}$$

Furthermore, since equation (5.2.21) is linear, different modes with different momentum k do not influence each other. When focusing on the evolution of a given mode, we can set the initial value as $h_{\rm sup}(k) = 1$.

Depending on its (comoving) momentum k, a mode in the super-horizon regime will re-enter the horizon during RD or MD. When $k > \mathcal{H}_{\rm eq}$, where $\mathcal{H}_{\rm eq}$ is the Hubble rate in the RD-MD equilibrium moment, the mode re-enters the horizon during RD; when $k < \mathcal{H}_{\rm eq}$, the mode re-enters during MD [4]. The value of the comoving momentum $k_{\rm eq}$ when a mode enters the horizon at the RD-MD equilibrium can be obtained by

[4] Even larger modes never enter the horizon, and they are not observables.

letting $k_{\rm eq} = \mathcal{H}(\eta_{\rm eq})$ in equation (5.2.14); then one obtain

$$k_{\rm eq} = \frac{2(2-\sqrt{2})}{\eta_{\rm eq}}\,. \tag{5.2.25}$$

The numerical value of the conformal time at RD-MD equilibrium is about $\eta_{\rm eq} \simeq 109.28\,{\rm Mpc}$ (see for example, section 17.6.5 in [48]), then $k_{\rm eq} \simeq 1.53 \times 10^{-2}\,{\rm Mpc}^{-1}$. Translating it to the corresponding value of frequency, $f_{\rm eq} = k_{\rm eq}/(2\pi)$, the result is about $f_{\rm eq} \simeq 1.66 \times 10^{-17}\,{\rm Hz}$ [48].

The ground-based detectors are sensitive to GWs whose frequency is in the range $10 - 10^3\,{\rm Hz}$, while the planned space-based detectors could detect GWs in the range $10^{-4} - 10^{-1}\,{\rm Hz}$. Thus from the point of view of direct observation, all detectors operate in the regime $f \gg f_{\rm eq}$, which corresponds to the primordial tensor perturbations that re-entered the horizon deep in the RD. For this reason, we would consider this kind of primordial tensor perturbations in this chapter.

In RD, equation (5.2.21) reduces to

$$h''(\eta,k) + \frac{2}{\eta}h'(\eta,k) + k^2 h(\eta,k) = 0\,, \tag{5.2.26}$$

which has the following analytic solution

$$h(\eta,k) = A_1\frac{\sin(k\eta)}{k\eta} + A_2\frac{\cos(k\eta)}{k\eta}\,. \tag{5.2.27}$$

However, with the initial condition of (5.2.23) and (5.2.24), we need to pick up the former solution, i.e.,

$$h(\eta,k) = h_{\rm sup}(k)\frac{\sin(k\eta)}{k\eta}\,. \tag{5.2.28}$$

This is the form of the transfer function for the tensor modes that re-enter the horizon during RD and then propagate to us.

5.3 AAC of the Inflationary SGWB

This section shows that inflationary SGWB possesses an angular correlation between the opposite directional GWs. This angular correlation is not contained in the astrophysical origin SGWB. This angular correlation results from the horizon re-entering of the super-horizon tensor mode. For simplicity, we assume that the background universe in which the primordial GWs propagates is homogeneous (i.e., the FLRW spacetime).

First, we write the sub-horizon mode of equation (5.2.28) in the form of

$$h(\eta, k) = \frac{e^{ik\eta} - e^{-ik\eta}}{2ik\eta}\,, \tag{5.3.1}$$

where we have set $h_{\rm sup}(k) = 1$. The tensor perturbation of (5.2.20) in comoving coordinates then becomes

$$h_{ij}(\eta, \mathbf{x}) = \int \frac{d^3k}{(2\pi)^3}\, \mathcal{A}_P(\eta, \mathbf{k})\, e^P_{ij}(\hat{\mathbf{n}})\, \left[e^{i(\mathbf{kx}+k\eta)} - e^{i(\mathbf{kx}-k\eta)}\right]\,, \tag{5.3.2}$$

where we have denoted $\mathcal{A}_P$ with

$$\mathcal{A}_P(\eta, \mathbf{k}) \equiv \frac{\mathtt{h}^{\rm pri}_P(\mathbf{k})}{2ik\eta}\,. \tag{5.3.3}$$

Then we change the variable of the wavenumber $\mathbf{k}$ to the frequency f by $\mathbf{k} = 2\pi f\hat{\mathbf{n}}$, with $f > 0$, therefore $d^3k = (2\pi)^3 f^2 df d^2\hat{\mathbf{n}}$. Also, we change the variable of f to $f' = -f$ for the first term in the bracket of (5.3.2) and rewrite the integral variable in terms of f; (5.3.2) becomes

$$\begin{aligned} h_{ij}(\eta, \mathbf{x}) = &\int_{-\infty}^{0} df \int_{S^2} d^2\hat{\mathbf{n}}\, \mathcal{A}_P(\eta, -f, \hat{\mathbf{n}})\, e^P_{ij}(\hat{\mathbf{n}})\, e^{-2\pi i f(\hat{\mathbf{n}}\cdot\mathbf{x}+\eta)} \\ &- \int_{0}^{\infty} df \int_{S^2} d^2\hat{\mathbf{n}}\, \mathcal{A}_P(\eta, f, \hat{\mathbf{n}})\, e^P_{ij}(\hat{\mathbf{n}})\, e^{2\pi i f(\hat{\mathbf{n}}\cdot\mathbf{x}-\eta)}\,. \end{aligned} \tag{5.3.4}$$

Next step is performing a similar change for the variable of $\hat{\mathbf{n}}$, $\hat{\mathbf{n}} = -\hat{\mathbf{n}}'$, in the first term of equation (5.3.4). We also change the convention of polarization basis

from the "plus-cross" convention ($P = +, \times$), defined in (5.1.2) and (5.1.3), to the "plus-minus" convention ($P = +, -$) which is defined by [5]

$$e^{\pm}_{ij}(\hat{\mathbf{n}}) \equiv e^{+}_{ij}(\hat{\mathbf{n}}) \pm i e^{\times}_{ij}(\hat{\mathbf{n}}) \,. \tag{5.3.5}$$

According to the definitions of "plus-minus" and "plus-cross" polarization basis, we have the relations:

$$e^{\pm}_{ij}(-\hat{\mathbf{n}}) = e^{\mp}_{ij}(\hat{\mathbf{n}}) \,. \tag{5.3.6}$$

Then, the first term of $h_{ij}(\eta, \mathbf{x})$ in equation (5.3.4) can be written as:

$$\text{First term} = \int_{-\infty}^{0} df \int_{S^2} d^2\hat{\mathbf{n}}\, \mathcal{A}_{-P}(\eta, -f, -\hat{\mathbf{n}})\, e^{-P}_{ij}(\hat{\mathbf{n}})\, e^{2\pi i f(\hat{\mathbf{n}}\cdot\mathbf{x}-\eta)} \,. \tag{5.3.7}$$

The final step is to change the comoving time to the cosmic time by the following relation:

$$\begin{aligned} \eta &= \int_{0}^{t_0} \frac{dt'}{a(t')} + \int_{t_0}^{t} \frac{dt'}{a(t')} \\ &\simeq \eta_0 + \frac{1}{a_0}(t - t_0) \,, \end{aligned} \tag{5.3.8}$$

where η_0 represents the age of the universe. The time interval $t_* \equiv t - t_0$ represents the duration of some observations. Because the observation time is far less than the age of the universe, the scale factor in the second integration can be treated as constant. The integrand of (5.3.7) now can be written as $\mathcal{A}_{-P}(t_*, -f, -\hat{\mathbf{n}})\, e^{-P}_{ij}(\hat{\mathbf{n}})\, e^{-2\pi i f \eta_0} e^{2\pi i f(\hat{\mathbf{n}}\cdot\mathbf{x}-t_*)}$. Performing the same change of variables for the second term in (5.3.4) and rewrite it in the form of plane wave expansion (5.1.1). The sub-horizon tensor mode of (5.3.2) can be written as

$$h_{ij}(\eta, \mathbf{x}) \to h_{ij}(t_*, \mathbf{x}) = \sum_{P=+,-} \int_{-\infty}^{\infty} df \int_{S^2} d^2\hat{\mathbf{n}}\, \mathsf{A}_P(f, \hat{\mathbf{n}}, t_*)\, e^{P}_{ij}(\hat{\mathbf{n}})\, e^{2\pi i f(\hat{\mathbf{n}}\cdot\mathbf{x}-t_*)} \,, \tag{5.3.9}$$

[5] Note that there is a possible confusing aspect of our notation for the polarization states. Remember that we only use the "plus-cross" convention in the following sections. Also, under this convention, when $P = \pm$, $-P$ will be $\mp$.

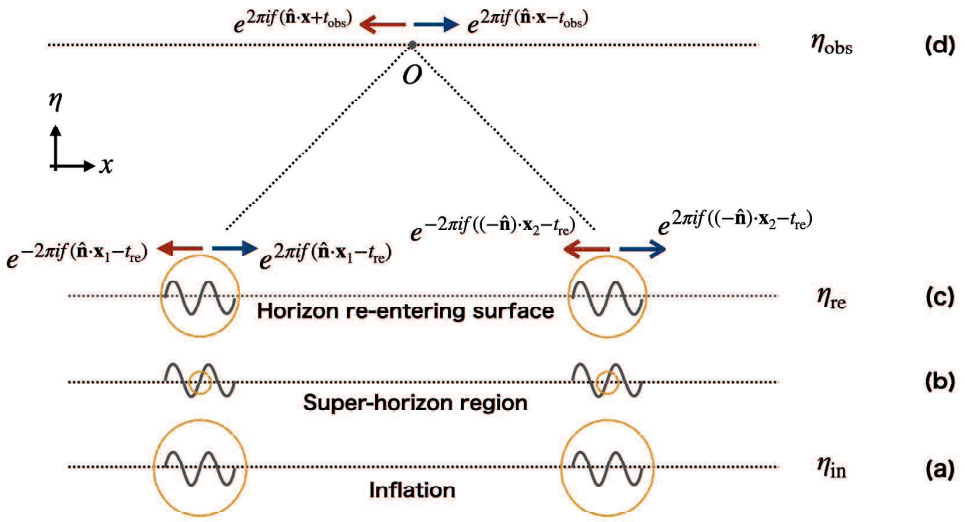

Fig. 5.3.1: An illustration of the AAC of inflationary SGWB. Circles represent the size of the comoving horizon of the universe. (a) and (b) Tensor perturbations are generated in inflation and thrown to the super-horizon region. (c) The super-horizon modes re-enter the horizon at some moment $\eta_{\rm re}$ during RD. At each point on the horizon re-entering surface, the plane-wave expansion modes of the tensor perturbation with opposite directions (the red and blue pair of arrows) have the same amplitude; each pair thus would form a standing wave. (d) The AAC in the inflationary SGWB is an angular correlation between the plane-wave expansion modes from the opposite directions $\hat{\mathbf{n}}$ and $-\hat{\mathbf{n}}$ (two different types of arrows at O).

where $\mathsf{A}_P(f,\hat{\mathbf{n}},t_*)$ is defined as

$$\mathsf{A}_P(f,\hat{\mathbf{n}},t_*) \equiv \mathcal{A}_P(f,\hat{\mathbf{n}},t_*)\, e^{-2\pi i f\eta_0} \tag{5.3.10}$$

with the relation of

$$\mathsf{A}_P(f,\hat{\mathbf{n}},t_*) = -\mathsf{A}_{-P}(-f,-\hat{\mathbf{n}},t_*)\, e^{-4\pi i f\eta_0}\,. \tag{5.3.11}$$

Relation (5.3.11) means that there is a correlation between plane wave expansion modes in the opposite directions $\hat{\mathbf{n}}$ and $-\hat{\mathbf{n}}$. We call this kind of correlation the *antipodal angular correlation (AAC)* (see Figure 5.3.1). The two-point correlation

function then becomes

$$\begin{aligned}\langle \mathsf{A}_P(f,\hat{\mathbf{n}}_1,t_*)\,\mathsf{A}^*_{P'}(f',\hat{\mathbf{n}}_2,t_*)\rangle &= \delta(f-f')\,\delta_{PP'}\,\delta^2(\hat{\mathbf{n}}_1,\hat{\mathbf{n}}_2)\,\frac{1}{2}S_h(f)\\ &\quad+\delta(f+f')\,\delta_{P(-P')}\,\delta^2(\hat{\mathbf{n}}_1,-\hat{\mathbf{n}}_2)\,\frac{1}{2}A_h(f)\,,\end{aligned} \tag{5.3.12}$$

where $S_h(f)$ represents the spectral density in (5.1.6) under the assumptions for normal SGWB; $A_h(f)$ is the spectral density which accounts for the anisotropic contribution of the AAC.

Using relation (5.3.11), one has

$$\begin{aligned}\langle \mathsf{A}_P(f,\hat{\mathbf{n}}_1,t_*)\,\mathsf{A}^*_{-P}(-f,-\hat{\mathbf{n}}_1,t_*)\rangle &\equiv \frac{1}{2}A_h(f)\\ &= -\langle \mathsf{A}_P(f,\hat{\mathbf{n}}_1,t_*)\,\mathsf{A}^*_{P}(f,\hat{\mathbf{n}}_1,t_*)\rangle\, e^{-4\pi i f\eta_0}\\ &= -\frac{1}{2}S_h(f)\,e^{-4\pi i f\eta_0}\,.\end{aligned} \tag{5.3.13}$$

Therefore we obtain the following relation between $S_h(f)$ and $A_h(f)$:

$$A_h(f) = -S_h(f)\,e^{-4\pi i f\eta_0}\,. \tag{5.3.14}$$

5.4 The Detectability of AAC

In this section, we discuss whether the AAC is observable in practice.

A note on our notations: for convenience, we will come back to use $h_P(f,\hat{\mathbf{n}})$ instead of $\mathsf{A}_P(f,\hat{\mathbf{n}})$ to denote the plane wave expansion components of the inflationary SGWB.

5.4.1 Strain Correlation Analysis

The basic idea of measuring an SGWB is correlating signals in different GW detectors operating simultaneously. [14]. For example, the outputs in the two detectors are:

$$s_1(t) = h_1(t) + n_1(t)\,, \tag{5.4.1}$$

$$s_2(t) = h_2(t) + n_2(t)\,, \tag{5.4.2}$$

where $h_{1,2}$ and $n_{1,2}$ represent detector's responses for GW signal and detectors' noises, respectively. The responses for the same GW signal in different detectors would correlate, but the noises usually would not. Therefore one may detect an SGWB by correlating the outputs $s_1(t)$ and $s_2(t)$, that is

$$\langle s_1(t)\, s_2(t)\rangle \approx \langle h_1(t)\, h_2(t)\rangle\,. \tag{5.4.3}$$

When we examine the detectability of the AAC in (5.3.12), one thing we should notice is that the variable $h_P(f,\hat{\mathbf{n}})$ [6] is *not* a variable that we directly observe. In practice, because the observational time is limited, say by an interval T, the observational quantity for $h_P(f,\hat{\mathbf{n}})$ is actually a quantity related to the observational time:

$$h_{P;T}(f,\hat{\mathbf{n}}) = \int_0^T dt\, h_P(t,\hat{\mathbf{n}})\, e^{2\pi i f t}\,, \tag{5.4.4}$$

where $h_P(t,\hat{\mathbf{n}})$ is the time domain stochastic background:

$$h_P(t,\hat{\mathbf{n}}) = \int_{-\infty}^{\infty} df\, h_P(f,\hat{\mathbf{n}})\, e^{-2\pi i f t}\,. \tag{5.4.5}$$

Substituting (5.4.5) into (5.4.4), we obtain

$$h_{P;T}(f,\hat{\mathbf{n}}) = \int_{-\infty}^{\infty} df'\, h_P(f',\hat{\mathbf{n}})\, W_T(f-f')\,, \tag{5.4.6}$$

where function $W_T(x)$ is defined by

$$W_T(x) \equiv \frac{\sin(\pi x T)}{\pi x}\, e^{i\pi x T}\,. \tag{5.4.7}$$

If the observational time T is infinite, then equation (5.4.6) would be the trivial relation $h_P(f,\hat{\mathbf{n}}) = \int_{-\infty}^{\infty} df'\, h_P(f',\hat{\mathbf{n}})\,\delta(f-f')$. However, because T can not be infinite, we see that rather than the Dirac delta function which picks up the value of $h_P(f',\hat{\mathbf{n}})$ only with $f=f'$, in (5.4.6) it is replaced by the function $W_T(x)$ that allows values of

[6] That is, the variable $\mathsf{A}_P(f,\hat{\mathbf{n}},t_*)$ in (5.3.12). Since the correlation relation of (5.3.12) is not related to the variable t_*, we omit it here.

$h_P(f', \hat{\mathbf{n}})$ in a frequency range of about $\Delta x \equiv |f' - f| \simeq 1/T$. The function $W_T(x)$ is thus called a *window function*. The appearance of the window function in the observational quantity $h_{P;T}(f, \hat{\mathbf{n}})$ is *inevitable* due to the limitation of observational time.

Using (5.4.6) and (5.3.12), we can compute the AAC in the strain correlations:

$$\langle h_{P;T}(f, \hat{\mathbf{n}})\, h^*_{-P;T}(-f, -\hat{\mathbf{n}})\rangle = \int_{-\infty}^{\infty} df' \, \frac{1}{2} A_h(f') \, |W_T(f - f')|^2 \, . \tag{5.4.8}$$

According to (5.3.14), we have

$$\langle h_{P;T}(f, \hat{\mathbf{n}})\, h^*_{-P;T}(-f, -\hat{\mathbf{n}})\rangle = \int_{-\infty}^{\infty} df' \, \frac{1}{2} S_h(f') \, |W_T(f - f')|^2 \, e^{-4\pi i f' \eta_0} \, . \tag{5.4.9}$$

In (5.4.9), the integrand contains a phase term that oscillates with a "period" of $\sim 1/(2\eta_0) \simeq 1/(2T_{\rm age})$, where $T_{\rm age}$ is the age of the universe and $1/T_{\rm age} \simeq 10^{-18}$Hz. Because of this phase term, unless the observational time is comparable to the universe's age, equation (5.4.9) approximates to zero. Therefore, the AAC is not measurable in the strain correlation.

5.4.2 Intensity Correlation Analysis

In the last subsection, we see that the contribution of antipodal correlation in the strain correlation is approximately zero due to the appearance of a fast oscillating phase factor $e^{-4\pi i f \eta_0}$. To get rid out of this phase factor, we consider the intensity correlations. The intensity correlation is considered for mapping an SGWB [57, 68]. Furthermore, because of the phase-decoherence effect during the propagation of GWs in the perturbed universe, Margalit, Contaldi, and Pieroni [51] have pointed out that only phase-incoherent methods (like the intensity map) are helpful to recover the angular dependence of primordial GWs. Indeed, according to (5.3.11), there is no additional phase factor in the antipodal correlation of the GW intensity:

$$I_P(f, \hat{\mathbf{n}}) = I_{-P}(-f, -\hat{\mathbf{n}}) \, , \tag{5.4.10}$$

where the intensity $I_P(f,\hat{\mathbf{n}})$ is defined with

$$I_P(f,\hat{\mathbf{n}}) \equiv |h_P(f,\hat{\mathbf{n}})|^2 \,. \tag{5.4.11}$$

On the other hand, like the "raw" strain of GW $h_P(f,\hat{\mathbf{n}})$, the intensity $I_P(f,\hat{\mathbf{n}})$ is not an observational quantity. The *observational intensity* $I_{P;T}(f,\hat{\mathbf{n}})$ is given by

$$I_{P;T}(f,\hat{\mathbf{n}}) = |h_{P;T}(f,\hat{\mathbf{n}})|^2 \,. \tag{5.4.12}$$

Using relations (5.3.3) and (5.3.10), we can explicitly write down $I_{P;T}(f,\hat{\mathbf{n}})$ as follows:

$$\begin{aligned} I_{P;T}(f,\hat{\mathbf{n}}) &= \int_{-\infty}^{\infty} df' \int_{-\infty}^{\infty} df''\, h_P(f',\hat{\mathbf{n}})\, h_P^*(f'',\hat{\mathbf{n}})\, W_T(f-f')\, W_T^*(f-f'') \\ &= \int_{-\infty}^{\infty} df' \int_{-\infty}^{\infty} df'' \, \frac{\mathfrak{h}_P^{\mathrm{pri}}(f',\hat{\mathbf{n}})\, \mathfrak{h}_P^{*\mathrm{pri}}(f'',\hat{\mathbf{n}})}{16\pi^2\, \eta_0^2\, f' f''}\, e^{-2\pi i (f'-f'')\eta_0}\, W_T(f-f')\, W_T^*(f-f'') \,. \end{aligned} \tag{5.4.13}$$

Because of the limitation of the ability of frequency resolution, the window function W_T (rather than a Dirac Delta function) appears in (5.4.13). As a result of this, the "undesired" phase factor $e^{-2\pi i(f'-f'')\eta_0}$ remains. Next, we consider the detectability of antipodal correlation in two categories of inflation models: standard inflation and anisotropic inflation.

- Standard inflation

As discussed in Section 4.4, primordial GWs are quantum fluctuations of the FLRW spacetime and are isotropic and homogeneous in the standard single-field slow-roll inflation model. We now examine whether we can construct an estimator of the observational intensity to detect the AAC.

First, let us consider the one-point function (i.e. the average) of the statistical quantity $I_{P;T}(f,\hat{\mathbf{n}})$:

$$\mathcal{I}_{P;T} \equiv \langle I_{P;T}(f,\hat{\mathbf{n}}) \rangle \,; \tag{5.4.14}$$

where the bracket $\langle ... \rangle$ denotes taking ensemble average, and Figure 5.4.1 explains

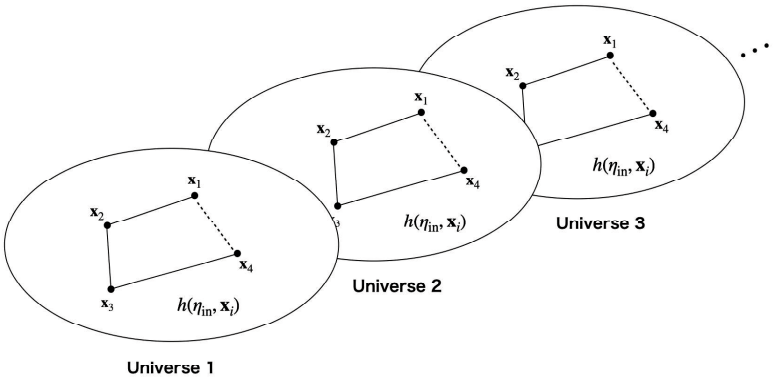

Fig. 5.4.1: The ensemble is an idealization consisting of many copies of a system. Each copy of the system represents a possible state that the system might be in. The ensemble average then means the average over these copies of the system. In our discussion of cosmological perturbations, the system is the whole universe.

its meaning. Under the standard assumptions of (4.4.2) about the primordial tensor perturbations, the one-point function does not have directional dependence, $\mathcal{I}_{P;T} \to \mathcal{I}_{P;T}(f)$:

$$\mathcal{I}_{P;T}(f) = \langle I_{P;T}(f, \hat{\mathbf{n}}) \rangle = \frac{\pi}{2} \int_{-\infty}^{\infty} df' \, \frac{P_{h,\rm in}(f')}{\eta_0^2 \, (f')^2} \, |W_T(f - f')|^2 \,, \tag{5.4.15}$$

and therefore, it is not a suitable estimator for revealing the directional dependence of the antipodal correlation.

Next, let us consider the two-point function, i.e., the *co-variance* $\Delta_I(\hat{\mathbf{n}}_1, \hat{\mathbf{n}}_2; f_1, f_2)$ of the observational intensities in two directions $\hat{\mathbf{n}}_1$ and $\hat{\mathbf{n}}_2$:

$$\Delta_I(\hat{\mathbf{n}}_1, \hat{\mathbf{n}}_2; f_1, f_2) \equiv \langle (I_{P;T}(f_1, \hat{\mathbf{n}}_1) - \mathcal{I}_{P;T}(f_1)) \, (I_{P';T}(f_2, \hat{\mathbf{n}}_2) - \mathcal{I}_{P';T}(f_2)) \rangle \,. \tag{5.4.16}$$

The co-variance in the antipodal directions is thus obtained with $\Delta_I(\hat{\mathbf{n}}, -\hat{\mathbf{n}}; f, -f)$:

$$\Delta_I(\hat{\mathbf{n}}, -\hat{\mathbf{n}}; f, -f) = \langle (I_{P;T}(f, \hat{\mathbf{n}}) - \mathcal{I}_{P;T}(f)) \, (I_{(-P);T}(-f, -\hat{\mathbf{n}}) - \mathcal{I}_{(-P);T}(-f)) \rangle \,, \tag{5.4.17}$$

and it reduces the correlations of the GW strain by the assumption of Gaussianity of

$h_P(f,\hat{\mathbf{n}})$:

$$\begin{aligned}\Delta_I(\hat{\mathbf{n}},-\hat{\mathbf{n}};f,-f) =& \langle h_{P;T}(f,\hat{\mathbf{n}})\, h^*_{(-P);T}(f,-\hat{\mathbf{n}})\rangle \langle h^*_{P;T}(f,\hat{\mathbf{n}})\, h_{(-P);T}(f,-\hat{\mathbf{n}})\rangle \\ &+ \langle h_{P;T}(f,\hat{\mathbf{n}})\, h^*_{(-P);T}(-f,-\hat{\mathbf{n}})\rangle \langle h^*_{P;T}(f,\hat{\mathbf{n}})\, h_{(-P);T}(-f,-\hat{\mathbf{n}})\rangle \\ =& |\langle h_{P;T}(f,\hat{\mathbf{n}})\, h^*_{(-P);T}(f,-\hat{\mathbf{n}})\rangle|^2 + |\langle h_{P;T}(f,\hat{\mathbf{n}})\, h^*_{(-P);T}(-f,-\hat{\mathbf{n}})\rangle|^2 ,\end{aligned} \tag{5.4.18}$$

where in the above deviation, we also used the reality condition (5.1.4).

In (5.4.18), the first term does not possess correlation; the second term is just the square of the strain correlation (5.4.9), and it vanishes due to the oscillating phase factor. Therefore, the co-variance of the observational intensity is approximately zero,

$$\Delta_I(\hat{\mathbf{n}},-\hat{\mathbf{n}};f,-f) \simeq 0 , \tag{5.4.19}$$

and thus, it is not a suitable estimator for detecting the AAC. Higher order functions are also of no use to detect the AAC because the property of Gaussianity reduces them to the correlation between GW strains. Therefore, we conclude that *under the standard inflation model, there is no suitable intensity estimator to detect AAC.*

- Anisotropic inflation

Apart from the standard scenario, some inflation models realized in the supergravity theory can brake the rotational symmetry [39, 40, 84, 79]. Under these models, primordial GWs can be statistically anisotropic, and the detectability of AAC is different from the standard inflation case. Here, we do not focus on specific anisotropic models but only notice that, in this case, the primordial power spectrum has a directional dependence [79], $P_{h,\mathrm{in}}(k) \to P_{h,\mathrm{in}}(\mathbf{k})$:

$$\langle \mathtt{h}^{\mathrm{pri}}_P(\mathbf{k})\, \mathtt{h}^{*\mathrm{pri}}_{P'}(\mathbf{k}')\rangle = (2\pi)^3\, \delta_{PP'}\, \delta^{(3)}(\mathbf{k}-\mathbf{k}')\, P_{h,\mathrm{in}}(\mathbf{k}) . \tag{5.4.20}$$

Therefore, unlike the standard inflation case, now the one-point function $\mathcal{I}_{P;T}$ has

directional dependence and is also free from the oscillating phase factor [7] :

$$\mathcal{I}_{P;T}(f,\hat{\mathbf{n}}) \equiv \langle I_{P;T}(f,\hat{\mathbf{n}})\rangle = \frac{\pi}{2}\int_{-\infty}^{\infty} df' \, \frac{P_{h,\mathrm{in}}(f',\hat{\mathbf{n}})}{\eta_0^2\,(f')^2}\,|W_T(f-f')|^2\,. \tag{5.4.21}$$

We can describe the anisotropy of $\mathcal{I}_{P;T}(f,\hat{\mathbf{n}})$ by its deviation $\delta\mathcal{I}_{P;T}(f,\hat{\mathbf{n}})$, defined with

$$\delta\mathcal{I}_{P;T}(f,\hat{\mathbf{n}}) \equiv \mathcal{I}_{P;T}(f,\hat{\mathbf{n}}) - \bar{\mathcal{I}}_{P;T}(f)\,, \tag{5.4.22}$$

where $\bar{\mathcal{I}}_{P;T}(f)$ is the averaged intensity over the full sky,

$$\bar{\mathcal{I}}_{P;T}(f) \equiv \frac{1}{4\pi}\int d^2\hat{\mathbf{n}}\,\mathcal{I}_{P;T}(f,\hat{\mathbf{n}})\,. \tag{5.4.23}$$

The antipodal angular correlation of the primordial GW strain (5.3.11) ensures that the one-point function $\mathcal{I}_{P;T}(f,\hat{\mathbf{n}})$ also possess an antipodal angular relation: $\mathcal{I}_{P;T}(f,\hat{\mathbf{n}}) = \mathcal{I}_{-P;T}(-f,-\hat{\mathbf{n}})$, and therefore, the deviation satisfies

$$\delta\mathcal{I}_{P;T}(f,\hat{\mathbf{n}}) = \delta\mathcal{I}_{-P;T}(-f,-\hat{\mathbf{n}})\,. \tag{5.4.24}$$

We thus conclude that under anisotropic inflation models, the inflationary SGWB *can* be distinguished from other components of the SGWB if we observe *(i) the non-vanishing anisotropies* $\delta\mathcal{I}_{P;T}(f,\hat{\mathbf{n}})$ *and (ii) their antipodal relation* (5.4.24).

5.4.3 Time-domain Analysis

In previous subsections, we discussed the detectability of the AAC by the correlations of the Fourier amplitude or the intensity and found that the detectability of the AAC in the standard inflation model is limited by the frequency limitation due to the finite observation time. In this subsection, we discuss the correlation between time signals and show that the time-domain analysis with a general assumption on the primordial GW spectrum can not detect the AAC.

[7] Notice that statistical homogeneity still holds, and thus $\delta(f-f')$ appears when we change the variable from wavenumber vector $\mathbf{k}$ to frequency f in (5.4.20).

First, we define the time domain correlation function $C(t_0, \tau, \hat{\mathbf{n}}_1, \hat{\mathbf{n}}_2)$ as

$$C(t_0, \tau, \hat{\mathbf{n}}_1, \hat{\mathbf{n}}_2) \equiv \langle h_P(t_0 - \tau/2, \hat{\mathbf{n}}_1)\, h_{P'}(t_0 + \tau/2, \hat{\mathbf{n}}_2)\rangle\,, \tag{5.4.25}$$

where t_0 and τ represent the start time and the duration of one observation, respectively. The time domain signal $h_P(t, \hat{\mathbf{n}})$ is the inverse Fourier transform of the stochastic variable $h_P(f, \hat{\mathbf{n}})$:

$$h_P(t, \hat{\mathbf{n}}) = \int_{-\infty}^{\infty} df\, h_P(f, \hat{\mathbf{n}})\, e^{-2\pi i f t}\,. \tag{5.4.26}$$

The standard contribution to the correlation function of an SGWB is coming from the same directions, $\hat{\mathbf{n}}_1 = \hat{\mathbf{n}}_2 (= \hat{\mathbf{n}})$. In this case, the correlation function becomes

$$\begin{aligned} C_S(\tau) \equiv C(t_0, \tau, \hat{\mathbf{n}}, \hat{\mathbf{n}}) &= \langle h_P(t_0 - \tau/2, \hat{\mathbf{n}})\, h_{P'}(t_0 + \tau/2, \hat{\mathbf{n}})\rangle \\ &= \delta_{PP'} \frac{1}{2} \int_{-\infty}^{\infty} df\, S_h(f)\, e^{2\pi i f \tau}\,. \end{aligned} \tag{5.4.27}$$

We see that $C_S(\tau)$ is independent of the start time t_0. Therefore, statistically, we can use the correlations $h_P(t - \tau/2, \hat{\mathbf{n}})\, h_{P'}(t + \tau/2, \hat{\mathbf{n}})$ for different values of t as samples to estimate the correlation function $C_S(\tau)$. The spectral density $S_h(f)$ then could be estimated by taking the short-time Fourier transform of $C_S(\tau)$.

On the other hand, the antipodal contribution to the correlation function is coming from $\hat{\mathbf{n}}_1 = -\hat{\mathbf{n}}_2 (= \hat{\mathbf{n}})$. The correlation function then becomes

$$\begin{aligned} C_A(t_0) \equiv C(t_0, \tau, \hat{\mathbf{n}}, -\hat{\mathbf{n}}) &= \langle h_P(t_0 - \tau/2, \hat{\mathbf{n}})\, h_{P'}(t_0 + \tau/2, -\hat{\mathbf{n}})\rangle \\ &= \delta_{P(-P')} \frac{1}{2} \int_{-\infty}^{\infty} df\, A_h(f)\, e^{-4\pi i f t} \\ &= -\delta_{P(-P')} \frac{1}{2} \int_{-\infty}^{\infty} df\, S_h(f)\, e^{-4\pi i f (\eta_0 + t_0)}\,, \end{aligned} \tag{5.4.28}$$

where, in the last line, we have used (5.3.14). This result is independent of the duration time τ. Therefore, we can use the correlations $h_P(t - \tau/2, \hat{\mathbf{n}})\, h_{P'}(t + \tau/2, \hat{\mathbf{n}})$ for different values of τ as samples to estimate the correlation function $C_A(t_0)$. The

discussion seems to be parallel to the standard one. However, due to the phase factor of $e^{-4\pi i f \eta_0}$, the antipodal correlation function $C_A(t_0)$ is extremely small compared with the standard one $C_S(\tau)$ and therefore makes it almost unmeasurable.

To clarify this point, let us compute the antipodal and the standard correlation functions for an explicit spectral density $S_h(f)$. We consider a power-law spectral density $S_h(f) \propto f^{-\alpha}$, where $\alpha \simeq 3$, which is a normal assumption for an inflationary SGWB. The antipodal correlation function (5.4.28) then becomes

$$C_A(t_0) = -\frac{1}{2}\int_{-\infty}^{\infty} df\, f^{-\alpha} e^{-ifT_*}\,, \tag{5.4.29}$$

where $T_* \equiv 4\pi(\eta_0 + t_0)$, and we have also assumed that the polarization states are $P = -P'$. Notice that in practice, the time domain signals actually do not contain the Fourier mode whose frequency is less than $f_{\min} = 1/\tau$, where τ is the time for some observations as defined above. In addition, the spectral density $S_h(f)$ should have an upper cut-off frequency $f_{\max}$ so that the total GW energy density is finite. Consequently, (5.4.29) becomes

$$C_A(t_0) = -\frac{1}{2}\int_{f_{\min}}^{f_{\max}} df\, f^{-\alpha} e^{-ifT_*}\,. \tag{5.4.30}$$

Because T_* has a large value, the integrand in (5.4.30) highly oscillates. To estimate this integral, we can use a method called the *steepest descent* [38]. Based on *Cauchy*'s theorem, which states that the value of the integral does not depend on the complex path taken, we select a new integration path $[f_{\min}, f_{\min} + ip] \cup [f_{\min} + ip, f_{\max} + ip] \cup [f_{\max} + ip, f_{\max}]$, where p is a real number, instead of the path $[f_{\min}, f_{\max}]$. Then the integral of $C_A(t_0)$ can be approximately evaluated by taking the limit of $p \to \infty$:

$$C_A(t_0) \simeq -\frac{i}{2}\left(e^{if_{\min}T_*}\int_0^{\infty} dp\,(f_{\min}+ip)^{-\alpha}\,e^{-pT_*} - e^{if_{\max}T_*}\int_0^{\infty} dp\,(f_{\max}+ip)^{-\alpha}\,e^{-pT_*}\right), \tag{5.4.31}$$

where the integral along the path $[f_{\min} + ip, f_{\max} + ip]$ vanishes for $p \to \infty$. Also, because of the integrand in (5.4.31) is suppressed by the function e^{-pT_*}, the main

contribution to the integration comes from the region around $pT_* < 1$. This is equivalent to $p < 1/T_* \ll f_{\rm min} < f_{\rm max}$. Therefore, the first integration in (5.4.31) can be estimated as:

$$\mathrm{Re}\int_0^\infty dp\,(f_{\rm min}+ip)^{-\alpha}\,e^{-pT_*} \simeq f_{\rm min}^{-\alpha}\int_0^\infty dp\,e^{-pT_*} = \frac{f_{\rm min}^{-\alpha}}{T_*}\,. \tag{5.4.32}$$

Performing the same estimation for the second integration, we can estimate $C_A(t_0)$ as

$$C_A(t_0) \simeq \frac{S_h(f_{\rm max})\sin(T_* f_{\rm max}) - S_h(f_{\rm min})\sin(T_* f_{\rm min})}{2T_*}\,. \tag{5.4.33}$$

On the other hand, the standard correlation function $C_S(\tau)$ takes its maximun value at $\tau = 0$. Taking this value in (5.4.27), we have:

$$C_S(\tau=0) = \frac{f_{\rm max}^{1-\alpha} - f_{\rm min}^{1-\alpha}}{2(1-\alpha)} = \frac{S_h(f_{\rm max})f_{\rm max} - S_h(f_{\rm min})f_{\rm min}}{2(1-\alpha)}\,. \tag{5.4.34}$$

Comparing (5.4.33) with (5.4.34), we see that the antipodal contribution is suppressed by a factor of $\sim 1/(f_{\rm min}T_*) = \tau/T_* = \mathcal{O}(10^{-10})$ compared with the standard contribution. Therefore, we conclude that the AAC is almost unmeasurable in the time-domain correlation analysis.

CHAPTER 6

Conclusion and Discussion

Searching the inflationary SGWB is one of the main goals in future GW observations. One of the main challenges in observing this kind of SGWB is isolating the inflationary component from other components, like those generated by unresolvable astrophysical sources. In this thesis, we derived a unique and universal angular correlation in the inflationary SGWB, the antipodal angular correlation, and discussed its detectability in actual observations.

The uniqueness of the antipodal correlation is that it results from the super- to sub-horizon transform of the primordial GWs, while the astrophysical GWs are in the sub-horizon regime all the time. The universal of the antipodal correlation is that it only depends on whether the exponential expansion (i.e., inflation) happens or not but not depends on exact inflation mechanisms. Therefore, as a distinguishable feature between the inflationary and astrophysical SGWB, it is worthwhile to investigate whether or not the antipodal angular correlation can be detected in observations.

Allen, Flanagan, and Papa [14] argued that the method of GW strain correlation can not detect the antipodal correlation due to the practically limited frequency resolution-ability. Furthermore, Margalit, Contaldi and Pieroni [51] pointed out that due to the phase-decoherence effect in the propagation of GWs under the perturbed universe, the only helpful methods in reconstructing the angular dependence in primordial GWs are phase-incoherent methods, for example, the intensity correlation. Concerning the above facts, we then investigated the detectability of the antipodal angular correlation in intensity correlation and time-domain analysis. The key results are as follows:

- Under the standard inflation scenario in which the generated primordial GWs are statistically isotropic and homogeneous, we can not find an appropriate estimator of intensity sensitive to the antipodal correlations due to the unavoidable fast oscillating phase factor in the intensity correlations.

- On the other hand, in inflation models with statistical anisotropy, there is a non-vanishing estimator, i.e., the one-point intensity function $\mathcal{I}_{P;T}(f, \hat{\mathbf{n}})$, which is sensitive to the antipodal angular correlation. The SGWB from anisotropic inflation can be distinguished from other components by measuring this one-point function.

- The direct cross-correlation of GW strains in time-domain can not detect the antipodal angular correlation because the antipodal contribution is much smaller than the contribution that comes from the same directions. The undetectability of the antipodal correlation by strain correlations is not a result of the limitation of Fourier analysis.

Therefore, we conclude that it is possible to distinguish the anisotropic inflationary SGWB from other types of SGWB by the unique antipodal angular correlation in the observed GW intensity. Nevertheless, several issues still need to be clarified in actual observations. The first one is the induced angular correlation in the inflationary SGWB. In our discussion of the detectability of the antipodal correlation, we assumed the background universe is homogeneous even in the propagation of primordial GWs. However, the real universe is not strictly homogeneous but is perturbed by matters like stars and galaxies. These perturbations will affect the phase and the magnitude of primordial GWs and therefore induce further angular correlations in the observed SGWB. We need to consider the proportional effect in actual measurements.

The second one is more subtle, and it concerns the explanation and replacement of the ensemble average in practice. In this thesis, we used the ensemble average to define the average of all statistical quantities, like the one-point function $\mathcal{I}_{P;T}$ of the observational intensity $I_{P;T}(f, \hat{\mathbf{n}})$: $\mathcal{I}_{P;T} \equiv \langle I_{P;T}(f, \hat{\mathbf{n}}) \rangle$. However, as mentioned in Subsection 5.4.2, because in the discussion of cosmological perturbations, our system

is the universe, and we do not have many copies of it. Therefore, in principle, we cannot measure the ensemble average. Nevertheless, under the ergodic hypothesis, the ensemble average can be replaced by a temporal average or a volume average, depending on the specific problem we involve. For example, when observing a perturbation over a given scale λ (where λ is assumed to be much smaller than the scale of the universe), we replace the ensemble average with an average over many different regions of size λ. If we want to check the AAC, which depends on directions, we need to replace the ensemble average in intensity with a temporal average over the GW signal. These issues in actual observations will be left for our future work.

REFERENCES

[1] Abbott, B. P. et al. (2016a). GW150914: First results from the search for binary black hole coalescence with Advanced LIGO. *Phys. Rev. D*, 93(12):122003.

[2] Abbott, B. P. et al. (2016b). Observation of Gravitational Waves from a Binary Black Hole Merger. *Phys. Rev. Lett.*, 116(6):061102.

[3] Abbott, B. P. et al. (2016c). Properties of the Binary Black Hole Merger GW150914. *Phys. Rev. Lett.*, 116(24):241102.

[4] Abbott, B. P. et al. (2017). Upper Limits on the Stochastic Gravitational-Wave Background from Advanced LIGO's First Observing Run. *Phys. Rev. Lett.*, 118(12):121101. [Erratum: Phys.Rev.Lett. 119, 029901 (2017)].

[5] Adams, M. R. and Cornish, N. J. (2014). Detecting a Stochastic Gravitational Wave Background in the presence of a Galactic Foreground and Instrument Noise. *Phys. Rev. D*, 89(2):022001.

[6] Ade, P. A. R. et al. (2014). Detection of B-Mode Polarization at Degree Angular Scales by BICEP2. *Phys. Rev. Lett.*, 112(24):241101.

[7] Ade, P. A. R. et al. (2015). Joint Analysis of BICEP2/$KeckArray$ and *Planck* Data. *Phys. Rev. Lett.*, 114:101301.

[8] Ade, P. A. R. et al. (2016). Planck 2015 results. XIII. Cosmological parameters. *Astron. Astrophys.*, 594:A13.

[9] Adshead, P., Afshordi, N., Dimastrogiovanni, E., Fasiello, M., Lim, E. A., and Tasinato, G. (2021). Multimessenger cosmology: Correlating cosmic microwave

background and stochastic gravitational wave background measurements. *Phys. Rev. D*, 103(2):023532.

[10] Aiola, S. et al. (2020). The Atacama Cosmology Telescope: DR4 Maps and Cosmological Parameters. *JCAP*, 12:047.

[11] Albrecht, A. and Steinhardt, P. J. (1982). Cosmology for Grand Unified Theories with Radiatively Induced Symmetry Breaking. *Phys. Rev. Lett.*, 48:1220–1223.

[12] Allen, B. (1988). The Stochastic Gravity Wave Background in Inflationary Universe Models. *Phys. Rev. D*, 37:2078.

[13] Allen, B. (1996). The Stochastic gravity wave background: Sources and detection. In *Les Houches School of Physics: Astrophysical Sources of Gravitational Radiation*, pages 373–417.

[14] Allen, B., Flanagan, E. E., and Papa, M. A. (1999). Is the squeezing of relic gravitational waves produced by inflation detectable? *Phys. Rev. D*, 61:024024.

[15] Allen, B. and Romano, J. D. (1999). Detecting a stochastic background of gravitational radiation: Signal processing strategies and sensitivities. *Phys. Rev. D*, 59:102001.

[16] Bar-Kana, R. (1994). Limits on direct detection of gravitational waves. *Phys. Rev. D*, 50:1157–1160.

[17] Bardeen, J. M. (1980). Gauge Invariant Cosmological Perturbations. *Phys. Rev. D*, 22:1882–1905.

[18] Bartolo, N. et al. (2022). Probing Anisotropies of the Stochastic Gravitational Wave Background with LISA.

[19] Bendat, J. and Piersol, A. (2010). *Random Data: Analysis and Measurement Procedures*. Wiley.

[20] Boileau, G., Christensen, N., Meyer, R., and Cornish, N. J. (2021). Spectral separation of the stochastic gravitational-wave background for LISA: Observing both cosmological and astrophysical backgrounds. *Phys. Rev. D*, 103(10):103529.

[21] Brustein, R., Gasperini, M., Giovannini, M., and Veneziano, G. (1995). Relic gravitational waves from string cosmology. *Phys. Lett. B*, 361:45–51.

[22] Buonanno, A., Maggiore, M., and Ungarelli, C. (1997). Spectrum of relic gravitational waves in string cosmology. *Phys. Rev. D*, 55:3330–3336.

[23] Buonanno, A., Sigl, G., Raffelt, G. G., Janka, H.-T., and Muller, E. (2005). Stochastic gravitational wave background from cosmological supernovae. *Phys. Rev. D*, 72:084001.

[24] Chowdhury, S. R. and Khlopov, M. (2021). The Stochastic Gravitational Wave Background from Magnetars. *Universe*, 7(10):381.

[25] Coleman, S. R. and Weinberg, E. J. (1973). Radiative Corrections as the Origin of Spontaneous Symmetry Breaking. *Phys. Rev. D*, 7:1888–1910.

[26] Contaldi, C. R. and Magueijo, J. a. (2018). Unsqueezing of standing waves due to inflationary domain structure. *Phys. Rev. D*, 98(4):043523.

[27] Damour, T. and Vilenkin, A. (2005). Gravitational radiation from cosmic (super)strings: Bursts, stochastic background, and observational windows. *Phys. Rev. D*, 71:063510.

[28] Dekel, A., Eldar, A., Kolatt, T., Yahil, A., Willick, J. A., Faber, S. M., Courteau, S., and Burstein, D. (1999). Potent reconstruction from Mark III velocities. *Astrophys. J.*, 522:1.

[29] Dodelson, S. and Schmidt, F. (2021). *Modern Cosmology*. Academic Press.

[30] Ferrari, V., Matarrese, S., and Schneider, R. (1999). Stochastic background of gravitational waves generated by a cosmological population of young, rapidly rotating neutron stars. *Mon. Not. Roy. Astron. Soc.*, 303:258.

[31] Fierz, M. and Pauli, W. (1939). On relativistic wave equations for particles of arbitrary spin in an electromagnetic field. *Proc. Roy. Soc. Lond. A*, 173:211–232.

[32] Grishchuk, L. P. (1974). Amplification of gravitational waves in an istropic universe. *Zh. Eksp. Teor. Fiz.*, 67:825–838.

[33] Grishchuk, L. P. (1993). Quantum effects in cosmology. *Class. Quant. Grav.*, 10:2449–2478.

[34] Gubitosi, G. and Magueijo, J. (2017). The phenomenology of squeezing and its status in non-inflationary theories. *JCAP*, 11:014.

[35] Gubitosi, G. and Magueijo, J. a. (2018). Primordial standing waves. *Phys. Rev. D*, 97(6):063509.

[36] Guth, A. H. (1981). The Inflationary Universe: A Possible Solution to the Horizon and Flatness Problems. *Phys. Rev. D*, 23:347–356.

[37] Hubble, E. (1929). A relation between distance and radial velocity among extra-galactic nebulae. *Proc. Nat. Acad. Sci.*, 15:168–173.

[38] Huybrechs, D. and Vandewalle, S. (2006). On the evaluation of highly oscillatory integrals by analytic continuation. *SIAM J. Numer. Anal.*, 44:1026–1048.

[39] Kanno, S., Kimura, M., Soda, J., and Yokoyama, S. (2008). Anisotropic Inflation from Vector Impurity. *JCAP*, 08:034.

[40] Kanno, S., Soda, J., and Watanabe, M.-a. (2010). Anisotropic Power-law Inflation. *JCAP*, 12:024.

[41] Kawamura, S. et al. (2021). Current status of space gravitational wave antenna DECIGO and B-DECIGO. *PTEP*, 2021(5):05A105.

[42] Kazanas, D. (1980). Dynamics of the Universe and Spontaneous Symmetry Breaking. *Astrophys. J. Lett.*, 241:L59–L63.

[43] Kibble, T. W. B. (1976). Topology of Cosmic Domains and Strings. *J. Phys. A*, 9:1387–1398.

[44] Kodama, H. and Sasaki, M. (1984). Cosmological Perturbation Theory. *Prog. Theor. Phys. Suppl.*, 78:1–166.

[45] Lemoine, M., Martin, J., and Peter, P. (2008). *Inflation Cosmology*. Springer.

[46] Linde, A. D. (1982). A New Inflationary Universe Scenario: A Possible Solution of the Horizon, Flatness, Homogeneity, Isotropy and Primordial Monopole Problems. *Phys. Lett. B*, 108:389–393.

[47] Maggiore, M. (2007). *Gravitational Waves. Vol. 1: Theory and Experiments*. Oxford Master Series in Physics. Oxford University Press.

[48] Maggiore, M. (2018). *Gravitational Waves. Vol. 2: Astrophysics and Cosmology*. Oxford University Press.

[49] Malhotra, A., Dimastrogiovanni, E., Fasiello, M., and Shiraishi, M. (2021). Cross-correlations as a Diagnostic Tool for Primordial Gravitational Waves. *JCAP*, 03:088.

[50] Mandic, V. and Buonanno, A. (2006). Accessibility of the pre-big-bang models to ligo. *Phys. Rev. D*, 73:063008.

[51] Margalit, A., Contaldi, C. R., and Pieroni, M. (2020). Phase decoherence of gravitational wave backgrounds. *Phys. Rev. D*, 102(8):083506.

[52] Martin, J., Ringeval, C., and Vennin, V. (2014). Encyclopædia Inflationaris. *Phys. Dark Univ.*, 5-6:75–235.

[53] Martinovic, K., Meyers, P. M., Sakellariadou, M., and Christensen, N. (2021). Simultaneous estimation of astrophysical and cosmological stochastic gravitational-wave backgrounds with terrestrial detectors. *Phys. Rev. D*, 103(4):043023.

[54] MATSUBARA, T. (2014a). *Physical Foundations of Cosmology I*. University of Tokyo Press.

[55] MATSUBARA, T. (2014b). *Physical Foundations of Cosmology II*. University of Tokyo Press.

[56] Misner, C. W., Thorne, K. S., and Wheeler, J. A. (1973). *Gravitation*. W. H. Freeman, San Francisco.

[57] Mitra, S., Dhurandhar, S., Souradeep, T., Lazzarini, A., Mandic, V., Bose, S., and Ballmer, S. (2008). Gravitational wave radiometry: Mapping a stochastic gravitational wave background. *Phys. Rev. D*, 77:042002.

[58] Mukhanov, V. F., Feldman, H. A., and Brandenberger, R. H. (1992). Theory of cosmological perturbations. Part 1. Classical perturbations. Part 2. Quantum theory of perturbations. Part 3. Extensions. *Phys. Rept.*, 215:203–333.

[59] Nariai, H. and Tomita, K. (1971). On the removal of initial singularity in a big-bang universe in terms of a renormalized theory of gravitation. 2. criteria for obtaining a physically reasonable model. *Prog. Theor. Phys.*, 46:776–786.

[60] Padmanabhan, T. (1993). *Structure formation in the universe*. Cambridge university press.

[61] Pan, Z. and Yang, H. (2020). Probing Primordial Stochastic Gravitational Wave Background with Multi-band Astrophysical Foreground Cleaning. *Class. Quant. Grav.*, 37(19):195020.

[62] Parida, A., Mitra, S., and Jhingan, S. (2016). Component Separation of a Isotropic Gravitational Wave Background. *JCAP*, 04:024.

[63] Penzias, A. A. and Wilson, R. W. (1965). A Measurement of excess antenna temperature at 4080-Mc/s. *Astrophys. J.*, 142:419–421.

[64] Pieroni, M. and Barausse, E. (2020). Foreground cleaning and template-free stochastic background extraction for LISA. *JCAP*, 07:021. [Erratum: JCAP 09, E01 (2020)].

[65] Poletti, D. (2021). Measuring the primordial gravitational wave background in the presence of other stochastic signals. *JCAP*, 05:052.

[66] Regimbau, T. (2011). The astrophysical gravitational wave stochastic background. *Res. Astron. Astrophys.*, 11:369–390.

[67] Regimbau, T., Evans, M., Christensen, N., Katsavounidis, E., Sathyaprakash, B., and Vitale, S. (2017). Digging deeper: Observing primordial gravitational waves below the binary black hole produced stochastic background. *Phys. Rev. Lett.*, 118(15):151105.

[68] Renzini, A. I. and Contaldi, C. R. (2018). Mapping Incoherent Gravitational Wave Backgrounds. *Mon. Not. Roy. Astron. Soc.*, 481(4):4650–4661.

[69] Rosado, P. A. (2011). Gravitational wave background from binary systems. *Phys. Rev. D*, 84:084004.

[70] Sachdev, S., Regimbau, T., and Sathyaprakash, B. S. (2020). Subtracting compact binary foreground sources to reveal primordial gravitational-wave backgrounds. *Phys. Rev. D*, 102(2):024051.

[71] Saikawa, K. and Shirai, S. (2018). Primordial gravitational waves, precisely: The role of thermodynamics in the Standard Model. *JCAP*, 05:035.

[72] Sandage, A. (1988). Observational tests of world models. *Ann. Rev. Astron. Astrophys.*, 26:561–630.

[73] Sarangi, S. and Tye, S. H. H. (2002). Cosmic string production towards the end of brane inflation. *Phys. Lett. B*, 536:185–192.

[74] Sato, K. (1981). First Order Phase Transition of a Vacuum and Expansion of the Universe. *Mon. Not. Roy. Astron. Soc.*, 195:467–479.

[75] Seto, N., Kawamura, S., and Nakamura, T. (2001). Possibility of direct measurement of the acceleration of the universe using 0.1-Hz band laser interferometer gravitational wave antenna in space. *Phys. Rev. Lett.*, 87:221103.

[76] Sharma, A. and Harms, J. (2020). Searching for cosmological gravitational-wave backgrounds with third-generation detectors in the presence of an astrophysical foreground. *Phys. Rev. D*, 102(6):063009.

[77] Siemens, X., Mandic, V., and Creighton, J. (2007). Gravitational wave stochastic background from cosmic (super)strings. *Phys. Rev. Lett.*, 98:111101.

[78] Smoot, G. F. (1999). COBE observations and results. *AIP Conf. Proc.*, 476(1):1–10.

[79] Soda, J. (2012). Statistical Anisotropy from Anisotropic Inflation. *Class. Quant. Grav.*, 29:083001.

[80] Starobinsky, A. A. (1979). Spectrum of relict gravitational radiation and the early state of the universe. *JETP Lett.*, 30:682–685.

[81] Starobinsky, A. A. (1980). A New Type of Isotropic Cosmological Models Without Singularity. *Phys. Lett. B*, 91:99–102.

[82] Ungarelli, C. and Vecchio, A. (2004). A Family of filters to search for frequency dependent gravitational wave stochastic backgrounds. *Class. Quant. Grav.*, 21:S857–S860.

[83] Wald, R. M. (1984). *General Relativity*. Chicago Univ. Pr., Chicago, USA.

[84] Watanabe, M.-a., Kanno, S., and Soda, J. (2009). Inflationary Universe with Anisotropic Hair. *Phys. Rev. Lett.*, 102:191302.

[85] Watanabe, Y. and Komatsu, E. (2006). Improved Calculation of the Primordial Gravitational Wave Spectrum in the Standard Model. *Phys. Rev. D*, 73:123515.

[86] Weinberg, S. (1977). *The First Three Minutes. A Modern View of the Origin of the Universe*. Basic Books.

[87] Weinberg, S. (2008). *Cosmology*. Oxford University Press.

[88] Yadav, J., Bharadwaj, S., Pandey, B., and Seshadri, T. R. (2005). Testing homogeneity on large scales in the Sloan Digital Sky Survey Data Release One. *Mon. Not. Roy. Astron. Soc.*, 364:601–606.